12-2012

Development of Patient Specific Predictive Treatment Margins to Account for Prostate Motion During Treatment Using Real-Time Intra Fraction Tracking

Michael Edward Howard
mhowar14@utk.edu

To the Graduate Council:

I am submitting herewith a dissertation written by Michael Edward Howard entitled "Development of Patient Specific Predictive Treatment Margins to Account for Prostate Motion During Treatment Using Real-Time Intra Fraction Tracking." I have examined the final electronic copy of this dissertation for form and content and recommend that it be accepted in partial fulfillment of the requirements for the degree of Doctor of Philosophy, with a major in Nuclear Engineering.

Laurence F. Miller, Major Professor

We have read this dissertation and recommend its acceptance:

Ronald E. Pevey, Lawrence H. Heilbronn, Dayakar Penumadu

Accepted for the Council:

Carolyn R. Hodges

Vice Provost and Dean of the Graduate School

(Original signatures are on file with official student records.)

Development of Patient Specific Predictive Treatment Margins to Account for Prostate Motion During Treatment Using Real-Time Intra Fraction Tracking

A Dissertation

Presented for the

Doctor of Philosophy

Degree

University of Tennessee, Knoxville

Michael Edward Howard

December 2012

ACKNOWLEDGEMENTS

I would like to first thank Dr. Laurence Miller, my major professor, for his guidance and help throughout this research. I have known Dr. Miller for over 20 years and I'm glad that I finally got an opportunity to work with him on such a worthwhile project. I would also like to extend my gratitude to Dr. Ronald Pevey, Dr. Lawrence Heilbronn and Dr. Dayakar Penumadu for agreeing to serve on my doctoral committee. In addition, I'm very thankful for all of the support and assistance that Dr. Mohammad Khan has given me over these past few years. His expertise in the field of medicine as well as medical physics has been invaluable to this research. A special thank you goes to my dosimetrist LuAnn Chambers. Her expertise in treatment planning made this process easier. A final thanks goes to my family. Without their support and encouraging words, none of this would have been possible.

ABSTRACT

Radiation therapy for prostate cancer has evolved over time. Intra-fractional motion of the prostate has been a clinical limitation in dose delivery. Reduced margins can lead to less toxicity to critical structures and an overall reduction in the risk of secondary cancers. Three models have been developed to predict prostate margins based on the first five fractions of treatment.

An 8^{th} order polynomial model is utilized with the 95% and 99% predictive lines indicating margins. This approach is applied to 24 patients. The maximum values as indicated by the predictive lines are used as the margins for the patient. The resultant margins are then compared with the remaining 34 fractions of treatment to determine whether a model is acceptable for clinical treatment.

The cumulative frequency distribution (CFD) is the second approach used in determining margins. The 95% and 99% data points are used as the predictive margins. The computed margins are then used to determine if the model is acceptable. A Bayesian model is the final approach. A posterior distribution is computed by implementing a uniform prior along with a Gaussian likelihood function. The 95% and 99% points along the distribution are utilized for margin determination.

Treatment plans are developed comparing the model that is most accurate versus a standard margin set that is in clinical practice. Individual margins derived by using the mathematical model varied significantly from patient to patient with ranges as follows (in mm): +x (1.5 to 2.5), -x (1.5 to 3.7), +y (1.5-5.4), -y (1.6 to 5.7), +z (1.5 to 4.2) and –z (1.5 to 4.6). The percentage of time the prostate moved outside of the individual patient margins based on the model was 0.86 +/- 1.07, 2.56 +/- 3.65 and 4.37 +/- 4.24 respectively.

Table of Contents

List of Tables

List of Figures

Chapter 1

Introduction

1.0 Prostate Cancer Therapy

Prostate cancer is one of the leading cancers diagnosed in men within the United States and is expected to affect 241,470 men of which 28,000 will die in 2012 (Siegel, 2011). Now, more than ever, patients have a variety of treatment options. These options include surgery, radiation therapy, brachytherapy, hormones and watchful waiting. The field of radiation oncology has led the way in technical advancement with regards to treating prostate cancer. Figure 1.1 represents a modern day linear accelerator. In the early 1990s, prostate cancer radiation therapy generally consisted of a 4-field (4 gantry angles) technique using standard cerrobend blocking (metal alloy material) around normal structures in order to minimize collateral damage to surround tissue. This method was effective but due to limitations by the equipment, a significant portion of the normal tissue received significant dose.

Figure 1.1 Varian TruBeam Linear Accelerator

The 4-field technique soon gave way to a 6-field technique that allowed slightly better normal tissue sparing but still gave significant dose to surrounding tissues. Around 2000, a new and more conformal technique called Intensity Modulated Radiotherapy (IMRT) was developed and quickly became the standard of care at many cancer centers around the United States. IMRT uses computerized Multi-Leaf Collimators (MLC) made of tungsten leaves placed in front of the beams path within linear accelerators in order to modulate the radiation beam pathway as it traverses through target tissues and normal tissues. In addition, better optimization algorithms were developed. The combination of the use of MLCs and better optimization algorithms allowed for increasing conformal dose distributions around the prostate and resulted in significant sparing of surrounding tissue. With such sharp dose gradients around the prostate, motion management became increasingly important and several Image Guided Radiotherapy Technologies (IGRT) also emerged simultaneously with the emergence of IMRT.

IMRT was a new concept in radiation therapy planning that had never been undertaken before. In conformal treatment planning, the physician draws the tumor, critical structures and blocks. The physician then inputs the desired dose to be delivered and then, the dose calculation is displayed quantitatively for approval by the physician. The physician can then change the blocking or relative radiation field weighting but has little other control over how much dose critical structures will receive. When utilizing IMRT, the process works the opposite. The algorithm utilizes inverse optimization in order to calculate dose. The physician still contours the critical structures and tumor but can now tell the computer how much dose to deliver to each structure, including the prostate. The algorithm works backwards in order to deliver the dose as prescribed to all structures. This process results in a significant number of “modulations” of the beam in order to achieve the desired results. In what used to be delivered in 6 ports (gantry angles), is now delivered in effectively 100-120 ports. The advent of IMRT allowed dose escalation in prostate therapy. Most clinicians using the standard 4/6 port technique delivered doses around 66 Gy to the prostate. Once the method of delivery switched to IMRT,

dose levels escalated to 78-81 Gy based on clinical evidence that increasing radiation doses to the prostate resulted in improved biochemical relapse free survival for patients (Zietman, 2005).

Once the use of IMRT became widespread, the issue of patient positioning became a significant issue in the oncology field. With such high modulation and the increase in prostate dose as a result, accurately positioning the patient became paramount. Standard practice in the radiation field included taking x-ray films weekly. This method utilized boney anatomy as an indicator if the patient was positioned correctly during treatment. Since most patients being treated have tumors that are soft tissue, weekly port films are inadequate as soft tissue is not well visualized with such devices.

1.1 The Need for IGRT in IMRT Treatments

The increase in dose and beam modulation requires improved tumor motion management and led to the development of IGRT devices, which focus on soft tissue alignment instead of bony tissue registration. IGRT utilizes a number of different methods in order to determine the location of the prostate. One of the first methods implemented in IGRT was ultrasound. Prior to each daily radiation treatment delivery (i.e. fraction of the total dose being delivered), the patient has an abdominal ultrasound study, which allows the clinician to accurately locate the prostate. The patient is then shifted into the correct position prior to treatment. This method has proven to be effective in most cases but has drawbacks including poor ultrasound images, not accounting for intra-fractional motion as well as position deformation with the ultrasound probe. An example of a clinical ultrasound system is shown in Figure 1.2.

Figure 1.2 Ultrasound System for Prostate Localization

The next development involved placing fiducial markers (small metallic objects) in the prostate for localization. A total of 3 gold fiducial markers (~ 7.5 mm in length) are inserted into the prostate prior to simulation for treatment (Figure 1.3). These markers are then tracked prior to each treatment. Computer software allows the alignment of the markers with the original CT scan in order to properly position the patient for treatment. This method has one significant limitation in that it is unable to track intra-fraction motion. The Calypso system has introduced a newer concept and uses 3 implanted radio transponders within the prostate that emit a radiofrequency of 10 Hz during radiation treatment delivery. These transponders allow the clinician to track prostate motion real time during an entire treatment session. Real time tracking data has shown that intra-fraction prostate motion can be very significant (Langen, 2008). Much like the fiducial markers, these transponders are placed prior to simulation. Once the patient is positioned on the table, these transponders relay positional information real time in 3-D. This data allows the treatment to be interrupted in

Figure 1.3 Gold Fiducial Markers

Figure 1.4 Calypso System

the event that the transponder falls outside an acceptable range. The following figure represents a Calypso imaging system. With the addition of IMRT along with IGRT, there has been a push in the clinical environment to reduce margins in order to minimize toxicity to critical structures (Gill, 2011). In prostate cancer, these critical structures include the rectum, bladder, penile bulb and femoral heads. Although all critical structures have limitations with respect to dose, the rectum and bladder are key in this process and tend to weigh more in clinical evaluation. One of the limiting factors in dose escalation to the prostate is the dose to these aforementioned structures. In the early history of radiation therapy, it was not uncommon to see 10 mm margins for the prostate in all directions with a 7.5 mm posterior border along the rectal wall. There are still a number of cancer centers that use these margins. Not only does this limit how high a dose can be given to the prostate, it also increases the potential for short term and long-term side effects to surrounding tissue (Gill, 2011). Normal tissue receiving dose 20-30 mm outside of the field is at an increased risk of complications.

There are protocols for prostate margins that have been greatly reduced from the days prior to IGRT. One clinical model is a 6 mm margin in all directions and a 4 mm margin posteriorly near the prostate/rectum interface. In addition, there is at least one model that suggests 2 mm margins all around may be possible with the use of real-time intra-fraction prostate tracking (Haise, 2008). The commonality with all of these models is that they assume margins are uniform across all patients and all related prostate motion will fall in between these margins during treatment delivery. In addition, these margins do not take into account the patient specific prostate motion, which is not currently fully understood. Clinicians continue to debate if prostate motion varies from patient to patient and if one can individualize and develop patient specific treatment margins based on individualized patterns of prostate motion. Thus, clinicians continue to use a wide range of treatment margins raging anywhere from 10-15 mm around the prostate to 5-10 mm posterior to the prostate.

1.2 Patient Prostate Tracking Data

The Calypso system uses three radio transponders to capture prostate motion. These transponders measure three vector coordinates (X,Y,Z) as a function of time (t). These transponders are placed in the prostate prior to simulation and in no set pattern. Figure 1.3 is an anatomical rendering of how the transponders are positioned in a typical patient. These markers are specially coated to reduce movement over the course of therapy. In Figure 1.4, the collection plate is positioned over the patient during their treatment delivery. The purpose of the collection plate is to receive the information from the transponders. The material on the plate is radiolucent in order to reduce the potential for beam attenuation. The plate remains in position for the entire period of treatment. The radio transponders transmit data at a rate of 10 Hz. The collection plate receives the transponder coordinate values during the entire length of the treatment. These values are transmitted in raw vector components. In order to analyze the motion, these data coordinates are then converted into the centroid or geometric center of the transponders. The following formula is utilized for this conversion.

$$\begin{aligned} C_x &= \left(X_1 + X_2 + X_3\right)/3 \\ C_y &= \left(Y_1 + Y_2 + Y_3\right)/3 \\ C_z &= \left(Z_1 + Z_2 + Z_3\right)/3 \end{aligned} \tag{1.1}$$

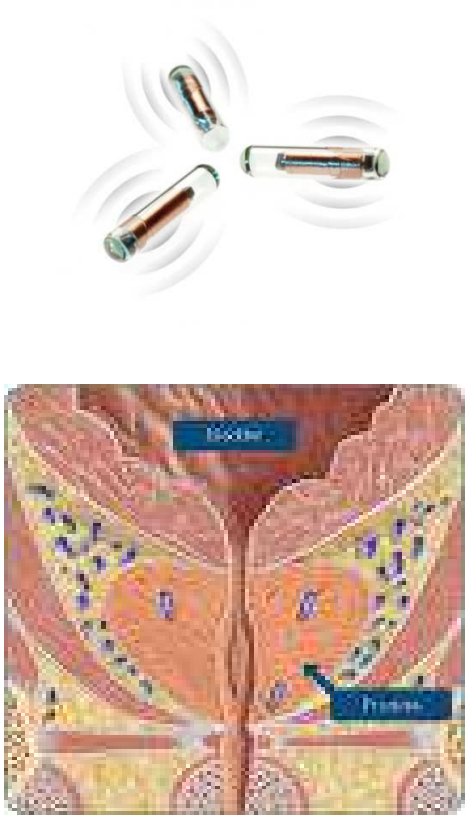

Figure 1.5 Calypso Transponders in Prostate Gland

Figure 1.6 Collection Plate Positioning During Treatment

Where (X,Y,Z) represent the corresponding vector component of the specific transponder. By converting the data into the centroid, any noise in the set can be minimized. The collection process will yield approximately 50,000 data points to analyze since it is captured at a 10 Hz frequency. On average, a treatment session for a patient will last from 6-12 minutes. The large variability in the time is related to the amount of interruptions that are necessary in order to reposition the patient (Howard, 2010), and the type of linear accelerator that is used during treatment delivery. In the initial work with Calypso, a threshold was set at 5 mm for 30 seconds. This corresponds to the centroid having a deviation of 5 mm lasting greater than 30 seconds in any one direction. When this occurs the beam is stopped and the patient is repositioned so that the transponders and the prostate can be realigned to the original isocenter (0,0,0). Once this is achieved, the radiation beam is restarted and the treatment session is either completed or interrupted again if the time and distance threshold of 5 mm lasting greater than 30 seconds is exceeded. After a period of time, it was determined that the criteria could be tightened. Clinicians decided on criteria that resulted in a reduced prostate motion cut off of only 3 mm. This did not result in delays of treatment delivery to patients and thus was considered clinically acceptable. All of the current patient files analyzed within this work follow the 3mm/30 sec intervention limits.

1.3 Scope of Research

Radiation therapy treatment of prostate cancer is centered on a population based model for treatment margins (Van Herk, 2000). All patients are assigned standard margins as determined by the radiation oncologist. The uniform margin approach does not account for a variety of biological and physiological functions that vary from patient to patient (Khan, 2012). In addition, it has been shown that prostate motion is patient specific and not uniform as previously thought (Howard, 2012). The possibility of patient specific margins has the potential to introduce significant dose sparing to critical structures while maintaining adequate coverage of the

prostate gland. In addition, the potential to reduce the overall risk of secondary cancers by reducing radiation dose to surrounding structures is a significant concern in the oncology community (Kleinerman, 2005).

This research will determine if prostate motion is predictable and if so, could one develop differential treatment margins for each patient based on patient specific patterns of prostate motion. The first step is to develop three different statistical models that model motion. These models include the Polynomial, Cumulative Frequency Distribution and a Bayesian approach. A model will be developed for each coordinate component (X,Y,Z). Using data from the first five fractions (i.e. model building), each model will then be tested using new data that the model has not previously seen (model validation step). Initial work on seven patients showed that five fractions are effective in developing a model (Howard, 2010).

The available data consists of 24 patients receiving radiation therapy at the Cleveland Clinic. This data is made available all patient identifiers removed in Excel format. A total of 31 patients were available for analysis. Once this data was received and reviewed, it was determined that only 24 were suitable for modeling. 7 of the 31 patients did not qualify for analysis as they had limited prostate tracking data that was not representative of a full course of IMRT. The patients reviewed in this study received a standard course of fractionated radiation therapy lasting for about 39 fractions depending on various clinical factors and the prescribed radiation dose. The prostate motion tracking data was collected with all patient identifiers being removed due to HIPPA compliance issues. The daily treatment process, setup and positioning follow standard practices and there are no known deviations encountered.

A comparison of each model will be made to determine which model is best at predicting motion. Once the preferred model is determined, it will be compared against two other clinical models. These models are the 2 mm model (Haise, 2008) and a clinically derived 6/4 mm model, which is based on clinical expertise. This comparison will be accomplished by comparing the predictive margins as determined by the models based on data from the first five fractions and assess their ability to predict future prostate motion for the remaining 34 fractions by scoring the percentage of prostate vector data points falling outside of the predicted margins. Criteria for the evaluating the performance of each model will be given in Chapter 2.

The preferred predictive model will then be compared with the 6/4 mm model in order to determine the effect on treatment planning. The Dose Volume Histogram (DVH) will be the method of evaluation to see if the predicted margins can reduce dose to the bladder and rectum. A treatment plan will be developed with the standard margins and then compared with an identical treatment plan developed with the predictive margins. This is accomplished by using a standard CT data set for a patient. A plan using each margin recipe will be developed based on the same anatomy. This will allow for a direct comparison of results. The DVH of the prostate, rectum and bladder will be evaluated at the dose values of 70 Gy, 50 Gy and 20 Gy. This comparison will determine the effective reduction in volume of the bladder and rectum across high and low dose ranges.

Chapter 2

Methods and Theory

2.0 Statistical Approach

As outlined in Chapter 1, there are three approaches taken in determining the predictive margins for patient treatments. In clinical radiation therapy, margins are assigned around critical structures in order to include gross as well as microscopic disease (i.e. disease that is outside of the prostate gland). This volume is referred to as the Planned Tumor Volume (PTV). These margins are constant and cannot be varied during the course of a treatment delivery. With this constraint in mind, the developed model must be able to make the margins as small as possible and still satisfy the criteria required for the treatment. The model must also estimate margins that are not too large. If the predictive margins are too large then the clinical impact of reducing standard margins is minimized or eliminated.

With these issues in mind, three separate models have been developed to predict patient specific margins for the series of patients utilized in this study. These models are the Polynomial, Cumulative Frequency Distribution (CFD) and Bayesian approaches. The details of the models and their application to this research will be explained in the following sections. Table 2.1 will be used in determining the performance of each model.

Table 2.1 Criteria for Model Evaluation

Percentage of Data Points Falling Outside of Clinical Margins	**Model Results**
0-5	Acceptable
5-10	Marginal
>10	Unacceptable

The basis for these values is determined by using current clinical standards for estimating accuracy in dose delivery (Bezjak, 2009). Radiation Therapy Oncology Group (RTOG) which is a national cooperative group funded by the National Cancer Institute (NCI), requires that 95% of the prescribed dose cover the PTV. This range defines the acceptable response of the model. The marginal range is established based on RTOG requirements that 99% of the PTV receive a minimum of 90% of the prescribed dose. When scoring a model, the assumption is that when any part of the prostate falls outside of the margin, it is not receiving the prescribed dose. This is valid when using 3-D techniques previously described. However, the use of IMRT reduces the probability of this occurring. The modulation of the radiation beam delivers dose in small fields within the PTV. This results in the potential for dose being delivered to the prostate even when a portion of the prostate falls outside of the margins. The impact of this effect is not evaluated in this research, thus the model provides an overestimation of under dosing that could result by using differential margins.

In the instance where the model predicts clinical margins that are not deliverable (i.e. too small), a threshold must be established within the model. This case arises when very little motion is displayed across the data sets. Routine radiation therapy delivery in the clinical setting has limitations such as setup error, laser alignment and immobilization. For the purpose of this research, this minimum margin will be set at 1.5 mm. Whenever the model determines margins less than 1.5 mm, the default of 1.5 mm will be used. This represents a small margin relative to current clinical standards that can still be delivered clinically. Future work might determine this value to be higher or lower but additional study is required and will be discussed in the chapter dealing with future work.

2.1 Beam Modeling

In order to deliver accurate dose with small fields, proper beam modeling is required. The predictive margin approach utilizes small margins and thus increases the need for accurate modeling. The modeling process is divided into four steps. The first section focuses on the beam spectrum. The energy spectrum defines the number of photons and associated energies in the range. There are sets of spectra data that have been published that allows the physicist to optimize the measured data. This process is critical in that the calculation of dose is dependent upon the modeled beam energy. The following figure represents the beam spectrum utilized in the planning process.

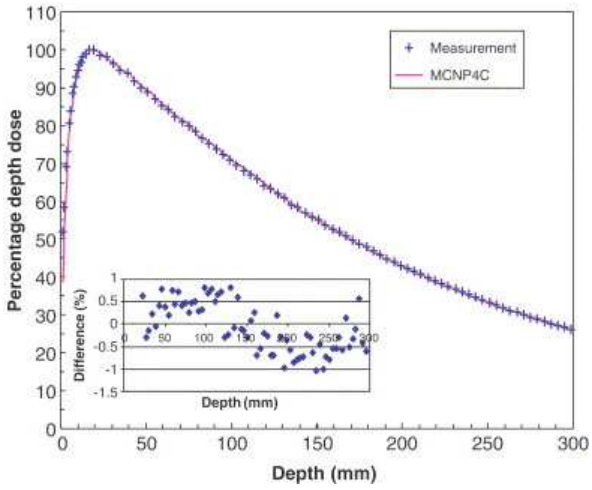

Figure 2.1 Beam Spectrum for Photons

Once the beam spectrum is modeled, the electron contamination must be added to the beam in order to account for the scatter effects from the linear accelerator head. This is accomplished by modeling the contamination as a modified exponential curve. At shallow depths, the dose is linear so as not to deliver excessive dose to the skin surface.

The next step in the modeling process is developing the in-field parameters. The flattening filter attenuation and off-axis softening are the two primary effects seen in field. The flattening filter attenuation has two effects on the beam. First, it changes the relative magnitude of the photon energy as a function of off-axis distance. In addition, it softens the beam as a function of off-axis distance. The off axis softening is modeled with the spectral off-axis softening parameter shown in equation 2.1.

$$W' = W_i * \left(\frac{1}{1 + \left(\frac{E_i}{E_{\max}} \right)} \right)^{OASP*\theta} \quad (2.1)$$

W is the defined as the spectral weight for bin "I" which has an effective energy E_i. Theta is the off-axis angle. It is calculated using the following equation.

$$\theta = a\tan\left(\frac{offaxisdist}{SAD} \right) \quad (2.2)$$

The off-axis distance is the distance between the central axis and the point of measurement that is orthogonal to the beam. As you increase the off-axis softening parameter, there is an increase in the horns associated with the profile of the beam. This is more pronounced near the surface of the beam.

Once the in-field parameters are modeled, the out of field parameters are determined. The out of field parameters have an impact in determining accurate dose delivery to patients. There are two primary components of the out of field model. The first factor is the effective source size parameter. The primary effect of source size is the modeling of the penumbra. This is accomplished by blurring the incident fluence model. The blurring kernel is modeled as a Gaussian function with the FWHM modeled as the

effective source size. If the effective source size is increased, the shoulders and base of the profile are more round. Decreasing the source size makes the profile more square.

The second parameter for out of field modeling is the flattening filter scatter source (FFSS). The flattening filter changes the shape of the primary beam but also is a source of secondary radiation. The FFSS models the scatter from the flattening filter. This effect is primarily seen in the tails of the distribution. The scatter is modeled with a Gaussian curve. There are two controls that can change this curve. The Gaussian height parameter determines the fraction of energy along the central axis that is due to scatter from the flattening filter. The Gaussian width parameter determines the width of the curve that is used to model the FFSS. Once the photon beam is properly modeled, the dose using the convolution algorithm can be calculated. The method of dose calculation is discussed in the following section.

2.1.1 Convolution Algorithm

Once the beam has been accurately modeled, it is necessary to calculate the dose at a given point in the patient. This is accomplished by using the convolution algorithm. This approach uses several components in order to calculate dose. The convolution algorithm is given in the following equation.

$$D(r) = \int \frac{\mu}{\rho}(r') \times \Psi(r') \times \mathrm{K}(r - r') d^3 r' \tag{2.3}$$

The factors in the equation above will be defined separately. It is important to note that the above equation shows no energy dependence. Each parameter has an energy dependence but the equation is a simplified version of the convolution algorithm. The energy has been integrated out over the range of spectral energies as determined in the modeling process.

The first factor in the integral is $\frac{\mu}{\rho}(r')$, which is defined as the mass attenuation coefficient. This coefficient is defined as the amount of energy removed from the primary radiation fluence per unit mass. The density of the patient determines the value of this spatially dependent factor. The primary energy fluence $\Psi(r')$ represents the photons per unit area. This factor represents the photon energy at a given point. In addition, the integral over the range of spatial locations gives the total photons in the volume irradiated. The product of the mass attenuation coefficient and the energy fluence is the referred to as the total energy released per unit mass (TERMA). TERMA is defined as the total amount of radiation at point (r') that is available for deposition in the patient.

The third factor is the convolution kernel $K(r-r')$. This is a polyenergetic dose-spread kernel. The values are determined by averaging the local beam spectrum of the radiation field. The photon energy range is determined in the modeling process by using the correct energy spectrum. The spectrum is spatially dependent so the kernel represents the energies at a given location in the patient. The convolution algorithm is the fundamental method with which dose at any given point in the patient is determined. Proper modeling is required in order to accurately determine dose using this method.

2.2 Polynomial Model

The initial model implemented in this research is the polynomial (Ott, 1988). The reasoning for this approach is that the polynomial is well understood, with well-defined mathematical properties. The computational process is straightforward and can be accomplished through a number of statistical programs. Polynomials have different orders and take the form in equation 2.4.

$$d = a_n t^n + a_{n-1} t^{n-1} + \ldots + a_2 t^2 + a_1 t^1 + a_0 \tag{2.4}$$

In the equation above, the dependent variable is the time (t) and the dependent variable is position (d). The above equation when plotted will generate a graph of motion over a given period of time. The coefficients of the polynomial can be determined taking the derivative of the polynomial at x_0. The variable x_0 is defined in equation 2.5.

$$x_0 = -\frac{a_{n-1}}{n a_n} \tag{2.5}$$

The fit of the equation is through the center portion of the data points. Due to the motion of the prostate, there is a scattering of the points. This reduces the effectiveness of this model if you consider only the fit equation. In order to account for the variations over the range of data, a prediction line is applied to the polynomial equation. The commercial software Sigma Plot version 11.2 is used for this model development. Figure 2.1 shows an example of displacement versus time graph that is a combined five treatment fractions.

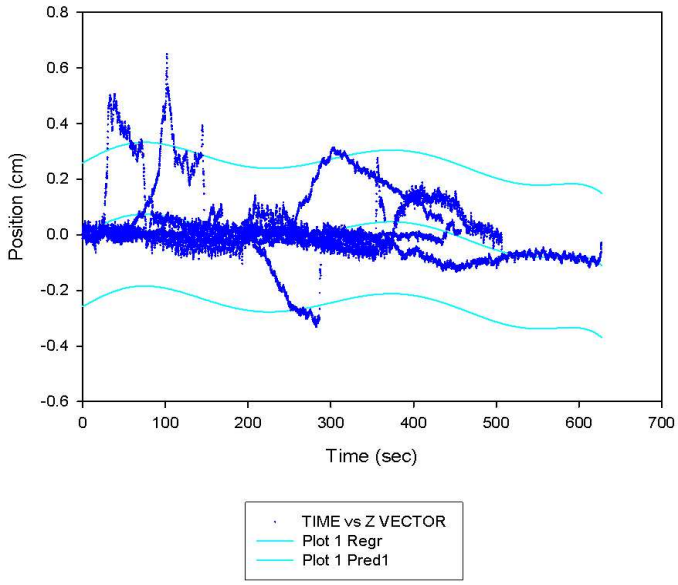

Figure 2.2 Displacement vs. Time

The center line on Figure 2.1 is representative of the polynomial fit and the two encompassing lines represent the 99% predictive lines applied to the data. Qualitatively it can be noted that the maximum and minimum points on the predictive lines are reactive to changes in the data pattern. These points are more pronounced when using a higher order polynomial model. Once it was determined that a polynomial model would be an appropriate choice for the initial work, determining the order is the next step.

Lower order polynomials are most often utilized in data analysis. However, in this case, a higher order polynomial might give significant improvement in the data analysis. Initially, 3rd and 4th order polynomials were analyzed. Due to the lower order, these polynomials have less of an ability to react to changes in the data. These changes include rectal gas along with other biological effects that result in quick displacement of

the prostate. These deviations which are generally on the order to 5 to 10 mm in magnitude can occur over just a few seconds or last for up to one minute. The lower order functions are unable to effectively model the inflection points during these changes. However, it was determined through several iterations of trial and error that higher order functions were able to better capture some of these deviations. Thus, an 8^{th} order polynomial proved to be the most effective approach.

In order to determine where a specific percentage of the data values fall, the predictive lines are utilized. The predictive line can be defined as the range where data values will fall within for repeated measurements. In this research, the maximum and minimum points of the predictive lines, in both the positive and negative axis for each of the three models is used for clinical margins. In radiation treatments, margins cannot be varied during delivery, so the maximum point is the appropriate value to use. In addition, using the maximum point of along the predictive line will give an extra margin to account for potential larger displacements in future treatment sessions. This is demonstrated in Figure 2.1. The formula for calculating the predictive line is given in equation 2.6 (SigmaPlot, 2009).

$$\hat{y}_0 \pm t(n-p-1)s\sqrt{1+X'_0(X'X)^{-1}X_0} \tag{2.6}$$

The variable y_o represents the 8^{th} degree polynomial model used in fitting the data for this model. The variables n is representative of the number of data points and p is the degree of the polynomial fit. The t value is a constant that is computed with a sixth order rational polynomial approximation (Sahai, 1974). The variable s is the variance about the regression, which is shown in equation 2.7.

$$s^2 = \sum_{i=1}^{n} \frac{\left(y_i - \tilde{y}_0 \right)^2}{n-1} \tag{2.7}$$

The variable X_0 is defined as the (p+1) and the X is defined as the n*(p+1) matrix. They are defined in the following equations 2.8 and 2.9 (Draper, 1981).

$$X_o' = \begin{bmatrix} 1 & x_0 & x_0^2 & . & x_0^p \end{bmatrix} \tag{2.8}$$

$$X = \begin{bmatrix} 1 & x_1 & x_1^2 & \dots & x_1^p \\ 1 & x_2 & x_2^2 & \dots & x_2^p \\ \dots & \dots & \dots & \dots & \dots \\ 1 & x_n & x_n^2 & \dots & x_n^p \end{bmatrix} \tag{2.9}$$

The variable x_0 is defined in equation 2.5. The x_n^p variable in equation 2.9 is associated with the corresponding polynomial. The polynomial fit is done to the cumulative set of data. The first five fractions are composed of five individual sets of data representing different days of treatment. There is a natural statistical variation over this period of time. By analyzing the five individual sets as one cumulative set, a better model can be developed.

2.3 Cumulative Frequency Distribution (CFD)

The polynomial model is a statistical model that can be utilized in predicting margins with respect to prostate motion. The polynomial approach takes data supplied by the user to determine coefficients in an equation that is then used to predict motion. The CFD model uses a different approach for margin prediction. Unlike the polynomial model, there is no mathematical model used in this approach. The data for the first five fractions is used to predict margins.

The CFD is a method that is straightforward and offers a different approach as seen with the polynomial approach. The cumulative probability for the first five fractions is ranked from lowest to highest in value (Tamhane, 2000). This can be seen in equation 2.10.

$$P_c = R_i / (N + 1) \tag{2.10}$$

R_i represents the position of the centroid at a given point. The (N+1) is the sampling number which is defined as the total number of points in the population of data. P_c is the ratio of the rank number and total number of data points. The margins are then determined by utilizing the 95% and 99% data points respectively. This method is a CFD that determines how much time the centroid spends at specified distances from the zero position. There are limitations to this method. As previously mentioned, the assumption is that all future motion will fall within the range of the first five fractions. This might not be realistic in most cases and thus could lead to reduced performance of the model.

In addition, depending on the size of the displacements that occur in every patient, the model may or may not be more accurate. A poor sampling of data over the first five fractions could lead to incorrect margins. As with the polynomial model, the 95% and 99% values are used in order to determine the clinical treatment margins.

The following figure is representative of a CFD dataset which is made up of the first five fractions of treatment. The graph is skewed in the negative direction. This shows for the given patient and vector model, there is a preference for the prostate to have a negative deflection during this time series. The units on the x-axis are in cm and indicated displacement. The model developed from this approach will show a significant variation in margins within the (+/-) directions.

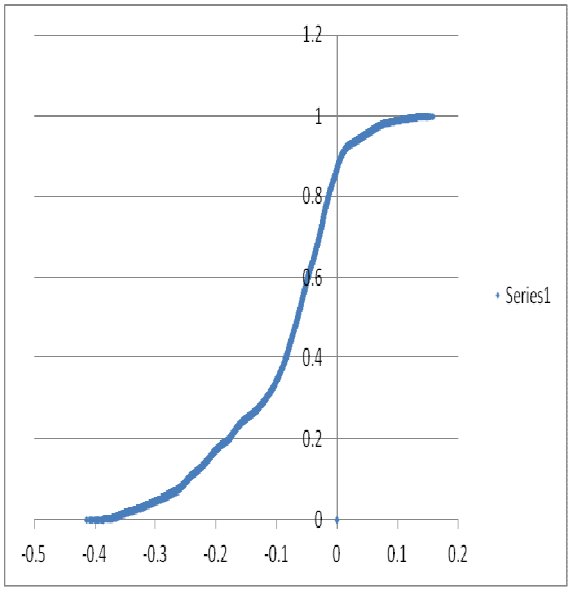

Figure 2.3 Cumulative Probability Distribution

2.4 Bayesian Model

In the previous sections, the polynomial model and CFD were discussed in detail. In order to validate these approaches and to determine if there is a better model available, the Bayesian approach was undertaken. Classical statistics is commonly used in research studies throughout all scientific fields. The Bayesian method is different yet offers comparable results with respect to the classical approach. The key advantage in Bayesian analysis is that it is possible to update information that is either learned or gathered. Updating allows the model to implement previously determined information into its calculation. This is accomplished by incorporating an informative prior into the posterior distribution. The prior can either be a constant or a distribution that is representative of previously gathered data. This is described by Bayes Theorem (Bolstad, 2007).

There are fundamental differences between the classical statistics and the Bayesian approach. Most commonly noted is what is known as Bayes Theorem. This theorem is the basis for the Bayesian approach and a fundamental understanding is necessary in order to implement this statistical method fully. The basis for Bayesian analysis is that given knowledge about a given situation or event, how much should that knowledge affect the predicted outcome of a future event. Figure 2.4 shows the impact that an informative prior can make on the data analysis. Even with this potential impact, choosing a non-informative prior can be beneficial as well. This is evident in that choosing the wrong prior or weighting information improperly in the prior can give rise to an inaccurate posterior density. This can lead to poor results. Careful consideration needs to be made if using an informative prior. Determining what data, how much to weight it and the proper function to model it with are all considerations. The use of a non-informative prior assigns equal weighting to previous knowledge and thus simplifies the analysis.

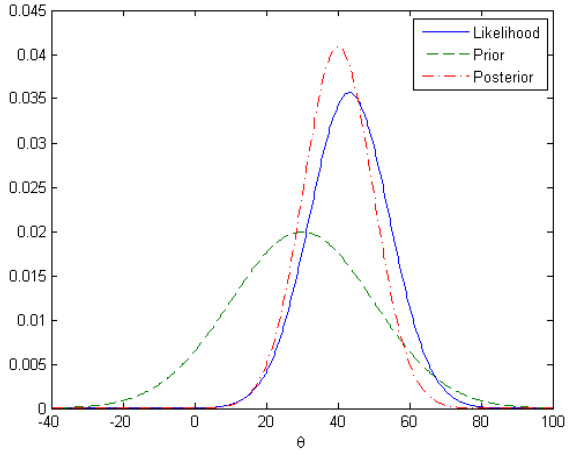

Figure 2.4 Graph of Posterior, Likelihood and Prior

The prior will be discussed in detail in the next section. Equation 2.11 is the basis for Bayesian analysis. This equation shows the relationship between the probability of A and B. Using the conditional probability of B given A and A given B.

$$P(A/B) = \frac{P(B/A)P(A)}{P(B)} \tag{2.11}$$

The variable P(A) represents the prior. The value P(B/A) represents the likelihood distribution for the data set. The choice for the likelihood function is important when determining the model that will best fit the data. The variable P(B) is a normalizing function for scaling purposes.

2.4.1 Posterior Distribution

The posterior distribution is an acceptable approach in developing predictive margins. The definition of the posterior distribution is the cumulative knowledge about all uncertain parameters. In this case it is the location of the prostate at any given point in time. This definition also includes unobserved and potential data as well. This is particularly important since we are predicting future motion based on multiple sets of data.

The prior can be an important component in the Bayesian approach. It has two basic forms, informative and non-informative. The non-informative approach assumes no information is known and its value or effect defaults to unity. This is a preferred method if very little is known about the data prior to analysis. However, choosing a non-informative prior limits the effectiveness of the posterior distribution if additional information is available. In this research, P(A)= 1.

The informative prior is a valuable tool in determining a more accurate posterior distribution (Winkler, 2003). There are a number of methods used in informative priors including conjugate and joint priors. The premise behind using this approach is that when prior information is known about the data set, it can be incorporated into the likelihood to yield better results. The mathematical issue with this approach is that the informed prior can skew datasets depending on how the data is obtained and how heavy it is weighted in the calculation. Its function is to supply information that may be available about a particular variable. This information often can lead to more finite results and thus reduce the uncertainty about the distribution.

In the case of this research, a non-informative prior is utilized. The reasoning behind this approach is two-fold. First, in the clinical world of medical physics, classical statistics dominates the field of study. The vast

majority of all research is conducted utilizing this approach. Incorporating a prior that provides little to no influence on the likelihood distribution allows for a wider clinical acceptance of this work. Second, there is a debate on how much prior information is actually known. Determining whether data gathered from other patients is considered prior information would need to be determined. More discussion on this topic will appear in the future research chapter of this dissertation.

The second factor of the posterior distribution is the likelihood function. The likelihood consists of a function that best models the datasets being analyzed. Through previous research (Khan, 2008), it has been shown that prostate motion is best described by a Gaussian distribution. With this in mind, it was determined that a Gaussian function is best suited to model the patient data sets (Ott, 1988). See equation 2.12.

$$\frac{1}{\sigma\sqrt{2\pi}} e^{\frac{-(x-\mu)^2}{2\sigma^2}} \tag{2.12}$$

Where σ^2 is the variance and μ is the mean of the dataset. The standard deviation (σ) is also factored into the function outside the exponential. The Gaussian function can be solved through an iterative process. The variable (x) represents the prostate displacement at any given point in time. The other parameters are computed based on the available data for the first five fractions of each patient.

The mathematical process used in the Bayesian approach involves the following steps. The first five fractions of data are taken for a specific patient. The mean, variance and standard deviation are calculated and entered

into the Gaussian function. In order to determine the range displacements that the prostate has over the patient population, a review of the entire 24 patients has been done. The vast majority of all patients will fall in the +5 to -5 mm displacement range. For the cases where this range does not encompass prostate motion for a particular patient, the range will be increased to account for the increase in motion. The Gaussian function is then computed over this range and normalized to the maximum point in order to generate the posterior distribution. Figure 2.3 is an example of the computed posterior distribution for a given patient.

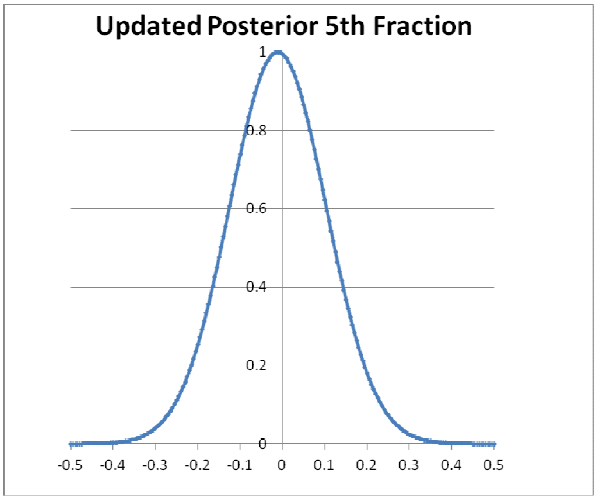

Figure 2.5 Posterior Distribution

The analysis is performed by taking the 95% and 99% data points in order to determine patient specific margins. This figure models only one vector component of a particular patient. In order to generate all the necessary clinical margins for treatment, two additional models will be developed for the corresponding vectors.

This approach will be compared to results obtained utilizing the polynomial model and the cumulative frequency distribution (CFD). The Bayesian model is a statistical approach that is useful in predicting treatment margins based on prostate displacement over the first five fractions. By analyzing multiple models, the potential to develop accurate patient specific margins is increased.

2.5 Correlation Analysis

The three statistical approaches presented here are useful in developing a model for predicting prostate motion. What the models do not do is determine why motion might be patient specific or what might lead to motion changes in a given model. In order to better understand the factors affecting prostate motion, the data will be analyzed and a correlation analysis will be done on several patients. This analysis is not meant to determine how all the physiological factors affect motion, rather this is meant to determine whether there is a correlation of motion across different vector models for a given patient or does each vector's motion pattern for a patient operate independently of another. This might be helpful in determining if one vector needs a uniform model across all patients or whether when a model fails, the reasoning behind it.

First, it is necessary to define how this analysis will be done. The most straightforward method to performing a correlation analysis of the data is the Pearson coefficient (Ott, 1988). The basic description of the Pearson coefficient is that it measures the overall strength of linear dependence between two variables. In the case of this research, the analysis involves the X / Y vector, X / Z vector and the Y / Z vector dependence. The equation used in calculating the Pearson coefficient is shown in equation 2.13 (SigmaPlot, 2009).

$$r_{xy} = \frac{\sum x_i y_i - n\overline{xy}}{(n-1)_{s_x s_y}} \tag{2.13}$$

Equation 2.13 can be defined as the co-variation of x and y divided by the unique variation in x and the unique variation in y. The variable x_i is time and y_i is position. The coefficient is a measure of how much the variables vary together as compared to how much they vary on an individual basis.

The Pearson coefficient can range in value from -1 to +1. If the coefficient has a value of 0, then the data series are considered to have no linear relationship or correlation. The closer the value comes to unity, the stronger the correlation exists between data sets. Although the Pearson coefficient does not give a full picture of the data, i.e. degree of dependence between the two sets of variables it is an effective tool in determining a relationship between data sets. Table 2.2 outlines the values of the Pearson coefficient and how they are interpreted for this research (Landis, 1977).

Table 2.2 Correlation Values

Correlation	**Positive**	**Negative**
Poor	0-0.2	-0.2-0
Fair	0.2-0.4	-0.2-(-0.4)
Moderate	0.4-0.6	-0.4-(-0.6)
Strong	0.6-0.8	-0.6-(-0.8)
Near Perfect	>0.8	>-0.8

The values listed in the table above are just estimates. There are no definitive numbers that are applicable in all cases. These values merely provide guidance in how to interpret the Pearson coefficient. Other analysis such as the modeling results will be helpful in determining the correlation between the various vector components.

In order to provide a complete analysis of the data, the p-value should be evaluated along with the Pearson coefficient. The p-value determines whether the probability of the data differing in the method presented happened by chance or is of statistical significance. The lower the p-value, the chance for a random happening is decreased. A threshold is set; below this threshold, the data is considered significant. This value varies between researchers and there is no definitive number but in the case of this research, it will be set to .01.

The correlation analysis will be done on three patients. The analysis will first be done on the five fractions used to determine the predictive margins. Then, an analysis will be completed on the remaining 34 fractions that are used in determining the success of the model. Comparing the results of the first five fractions versus the remaining fractions could provide insight to why a model might pass or fail. Also, this analysis might allow a better understanding of whether a particular vector component (X,Y,Z) is completely independent of other vectors. This is helpful in determining if a universal margin approach is warranted. In addition, this analysis will help in determining whether there is a correlation between any two vector components (Khan, 2012). This can result in a better understanding of prostate motion as well as better methods in developing predictive margins. These results will be presented in Chapter 3.

Chapter 3

Results

3.0 Overview of Results

The results discussion will be divided into several sections in order to facilitate discussion and analysis of the different models. The first section will focus on the Polynomial approach. The second section will focus on the Cumulative Frequency Distribution and then followed by the Bayesian model. Each section will discuss the general methods of each model, clinical margins generated and the overall performance of the model versus other clinically accepted approaches.

The following section will compare and contrast all three predictive models. Included in this comparison will be a recommendation of the best model for clinical implementation. The recommendation will be based on model performance as determined by Table 2.1 and the associated clinical margin evaluation. There will be a final section dedicated to reviewing the correlation analysis. The correlation analysis will be discussed for several patients and any findings or recommendations will be addressed.

3.1 The Polynomial Model

The Polynomial approach as described in Chapter 2 has been applied to the group of 24 patients that were obtained for this research. Tables 3.1 and 3.2 summarize the margins that were developed using the 95% and 99% predictive lines across all 24 patients.

Table 3.1 Clinical margins (in millimeters) for the Polynomial model utilizing the 95% predictive line.

Patient	**+X**	**-X**	**+Y**	**-Y**	**+Z**	**-Z**
101	1.5	1.5	2.4	2.9	2.7	3
102	1.5	3	1.5	1.5	2	2.1
103	2	1.5	3.5	5.5	2.5	5.2
106	1.5	1.5	1.6	3.1	2	3.5
108	1.5	1.5	5.5	2	4.5	1.8
109	1.5	1.5	2.5	2.3	3.5	3.2
110	1.6	1.5	3	1.7	2.9	1.9
111	1.5	1.5	1.5	3.5	1.5	1.9
112	1.5	1.5	2.5	3.1	5	3
113	2.1	1.5	1.5	1.5	1.5	1.5
114	1.5	1.5	3	1.6	2.4	1.9
115	1.5	1.5	1.5	3.5	1.8	3.2
116	1.8	1.5	2.1	3.1	3.2	4
117	1.5	1.5	5	5.7	4.3	4
118	1.5	1.5	1.5	2.7	1.6	3
119	1.5	1.8	1.5	1.8	2.8	3.3
120	1.5	1.5	2.4	2.4	2.6	3
123	1.9	2.2	3.5	2.7	1.5	2.7
124	1.5	1.5	1.5	1.5	1.5	2.3
125	1.9	1.5	3.4	2.9	3.1	2.4
126	1.5	1.5	2	2.5	1.5	2.3
129	1.5	1.5	2.3	1.5	1.9	2.5
130	2.2	1.5	2.4	2.8	2.3	3.1
131	1.9	1.5	1.8	1.5	3.4	1.8
Mean	1.62	1.60	2.47	2.64	2.57	2.77
S. Dev	0.23	0.33	1.09	1.13	1.01	0.87

Table 3.2 Clinical margins (in millimeters) for the Polynomial model utilizing the 99% predictive line.

Patient	**+X**	**-X**	**+Y**	**-Y**	**+Z**	**-Z**
101	1.5	1.5	3.4	3	3.4	3.4
102	1.6	3.5	1.5	1.7	2.3	2.5
103	2.2	1.5	4.2	6.3	3.1	5.8
106	1.5	1.5	2.1	3.7	2.7	4.3
108	1.5	1.5	6	2.6	4.9	2.3
109	1.5	1.5	3.2	2.9	4.3	4
110	1.7	1.5	3.5	2.2	3.6	2.4
111	1.5	1.5	2	1.9	1.6	2.2
112	1.5	1.5	3.2	3.6	5.8	3.8
113	1.5	2.4	1.5	1.5	1.5	3.5
114	1.5	1.5	3.5	2.1	3.2	2.4
115	1.5	1.5	1.9	3.8	2.3	3.8
116	2.1	1.5	2.5	3.6	4	4.7
117	1.5	1.5	6.4	7	5.2	4.9
118	1.5	1.5	1.5	3.1	2	3.5
119	1.5	2	1.5	2.1	3.4	4
120	1.5	1.5	2.9	3	3.4	3.8
123	2.4	2.8	4.4	3.3	1.5	2.8
124	1.5	1.5	1.5	1.5	1.5	2.4
125	2.1	1.5	4.1	3.7	3.6	2.4
126	1.7	1.7	2.3	2.8	1.8	2.5
129	1.5	1.5	2.7	2.1	1.9	2.6
130	2.3	1.5	2.9	3.3	2.9	3.8
131	2	1.7	2.3	1.7	3.5	2.3
Mean	1.64	1.80	3.03	3.12	2.95	3.47
S. Dev	0.30	0.50	1.34	1.35	1.21	0.98

As previously discussed, a 95% and 99% predictive line is applied to the 8^{th} order fit. These lines are used in determining the clinical margins. Since margins are not adjustable during the actual treatment delivery, only the maximums in either the positive or negative direction will be used in defining the clinical margins. Included in the summary of the patients is the associated mean and standard deviation for the entire population. This will be discussed in detail for each vector model. The corresponding coefficients to the 8^{th} order fit are available in the appendix for review.

3.1.1 Polynomial, X-model

The X-vector represents lateral motion of the prostate. In general, this direction has less movement than the other vectors. Based on the results in the previous tables, the mean for the 95% prediction line is 1.62 for the (+X) direction and 1.6 for the (–X) direction. The corresponding standard deviations are 0.23 and 0.33 respectively. This is indicative of data that has very little motion over the range of values. In this instance, the cumulative data used in computing margins for all patients is 548,249 points. This gives enough data for a statistical analysis. When the 99% predictive line is applied to the same group of patients, the margins increase. The mean is 1.62 for the (+X) direction and 1.8 for the (-X) direction. The associated standard deviations are 0.3 and 0.5. This shows an increase in predicted motion between the two approaches.

It is evident from the margins that the prostate motion is small relative to current clinically accepted treatment margins across most patients. As mentioned earlier in Chapter 2, when the model estimates a margin less than 1.5 mm, the threshold will be exceeded for clinical delivery and thus a 1.5 mm value will be assigned in that instance. From a review of the above tables, this occurs approximately 70% of the time with respect to the X-model. This is expected based on the mean and standard deviation values. Figures 3.1 and 3.2 represent the Polynomial X-model for two of the 24 patients presented for review.

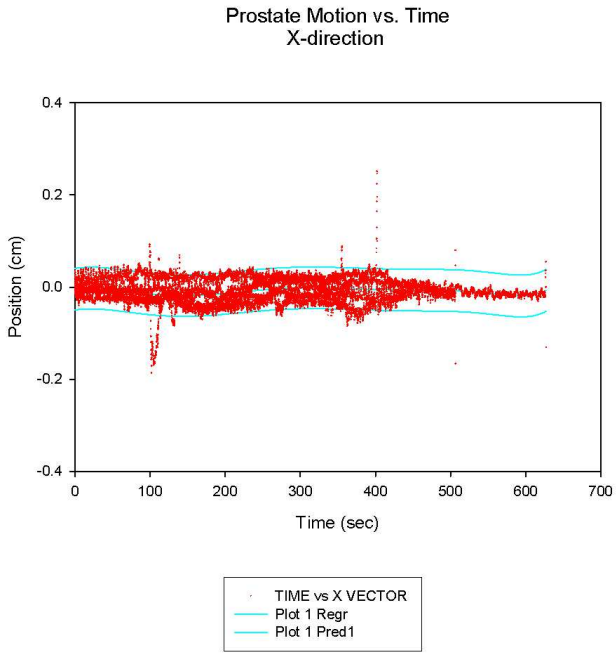

Figure 3.1 Polynomial fit for the X-model, CCF 101, 95% Predictive Line

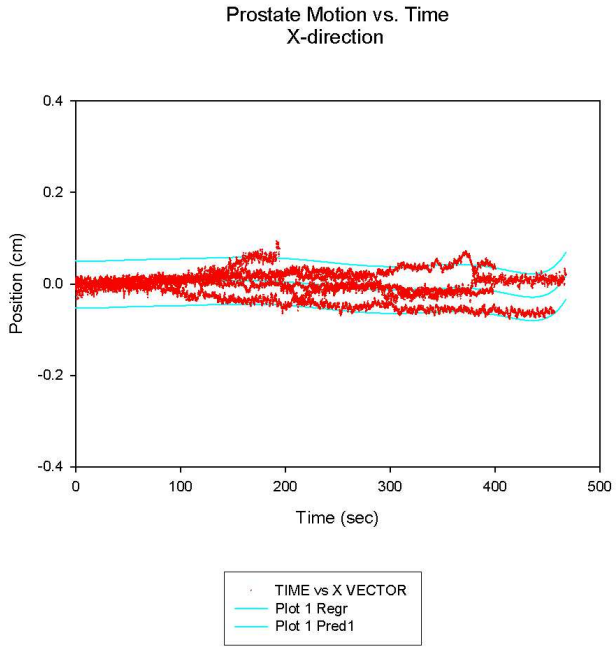

Figure 3.2 Polynomial fit for the X-model, CCF 115, 95% Predictive Line

These figures demonstrate the pattern of motion over the first five fractions for patient CCF 101 and 115 respectively. The one similarity between the two figures is that there is a lack of motion in the lateral direction. The resulting clinical margins are 1.5 mm in both cases. The lack of motion in the lateral plane is not unexpected based on how the prostate sits in the pubic region along with the ligament structure that holds the prostate in place.

Based on the results shown, it is reasonable to infer that a uniform model across all patients might be the best course in determining clinical margins for the X-model. Approximately 70% of patients are being assigned margins of 1.5 mm. There are several patients that exceed 2 mm in one direction. However, given that the polynomial model consistently estimates tight margins with respect to current clinical margins, it appears that the 1.5 mm approach is a sufficient starting point. Uniform margins for the X-model will be discussed further in future research.

The next step in determining the effectiveness of this approach is to validate the model. Validating the model is accomplished by taking the data from the remaining 34 fractions and comparing it with the treatment margins developed. An Excel macro was developed where the predictive margins developed from the 8^{th} order polynomial fit are applied to the remaining data. The data points are either scored as falling within the treatment margin or falling outside the treatment margin. The values in Table 2.1 are used to determine if the model performed acceptable, marginal or unsatisfactory. In addition, current clinically accepted treatment margin models are shown as well for a direct comparison. These models include the uniform 2 mm margin model along with the 6 mm in all directions and 4 mm posterior model. These models were presented in detail in Chapter 1. Table 3.3 represents the summary of the performance of the model over the 24 patients.

Table 3.3 Summary of Comparisons between Accepted Clinical Models and the Polynomial Model for the X-vector. Values indicate % of data points falling outside the clinical margins.

Patient	**2 model**	**6/4 mm**	**Poly 95**	**Poly 99**
101	.015	0	.024	.024
102	5.91	0	1.4	.58
103	0	0	.16	.16
106	2.1	0	3.3	3.3
108	.02	0	.96	.96
109	.05	0	1.9	1.9
110	1.24	0	3.4	3.2
111	.42	.04	1.3	1.30
112	.68	0	1.8	1.8
113	0	0	0	0
114	.02	0	.02	.023
115	0	0	0	0
116	3.4	0	8.5	6.2
117	2.8	0	7.2	7.2
118	3.4	0	3.5	3.5
119	2.8	0	4.9	2.8
120	0	0	0	0
123	2.8	0	3	2.6
124	.23	.07	1.2	1.2
125	.75	0	.91	.63
126	3.7	0	3.1	2.9
129	0	0	0	0
130	.04	0	0	0
131	.16	0	.23	.16

The 2 mm model scored acceptable across all patients but one. Patient CCF 102 was the only patient to fall outside the 5% threshold. The majority of patients fell below the 3% value. The 6/4 mm model had no data falling outside the 5% value. The lack of data points falling outside the threshold is not the best result. These results indicate that we are irradiating too much normal tissue. This leads to higher complication rates and a greater potential for secondary cancers. The fact that almost no data points fall outside of the margin is not a preferred approach. There needs to be a balance between effective margins and a motion management of the prostate.

The Polynomial model is broken down into the 95% and 99% predictive lines. Tables 3.1 and 3.2 break down the corresponding margins for each approach. In some instances the margins change significantly (> .8 mm) between these two models and other times the change is minimal (<.3 mm). When the predictive margins are applied to the group of patients, the results are quite different than the other two clinical margin approaches. The majority of the margins are in the 1.5-1.8 mm range. This offers a reduction in normal tissue that will be irradiated during treatment. When the 99% predictive line is applied, no patient fails in meeting either the acceptable or marginal criteria. Margins are slightly increased as seen in Table 3.2. This increase is expected based on using the 99% data point. Determining when one model should be applied over another is not a definitive process and will be discussed further in the future work section.

A complete review of Table 3.3 shows that the X-model for the Polynomial approach is effective in predicting margins for future treatment fractions. In the case of the 95% model, only one patient is unacceptable. No patients are unacceptable when using the 99% approach. There is a reduction in treatment volume when using the Polynomial model when compared to the 6/4 mm model. This reduction is dependent on the size of the predictive margins and varies by patient. The treatment planning process and Dose Volume Histogram (DVH)

analysis will be discussed in Chapter 4. The predictive margins are only one aspect of this analysis. It is also necessary to show that the clinical impact is meaningful and will result in an effective treatment planning result.

3.1.2 Polynomial, Y-model

The Y-vector represents motion in the anterior / posterior directions. This motion can be greatly influenced by physiological processes such as rectal gas and bladder fill rate. Unlike the X-vector where there was very little motion, the motion in the anterior / posterior direction is more pronounced. Given the nature of some of these processes, the motion pattern will exhibit various peaks throughout the treatment process. In order to model the motion effectively and obtain accurate treatment margins, the model will need to be responsive by taking into account even small variations in motion.

The results in Table 3.1 indicate the motion is more pronounced than the X-vector. The mean for the 95% approach is just less than 2.5 mm and the 99% model results in a mean value of 3 mm. These values represent anterior motion. The posterior motion for the 95% and 99% models is 2.6 mm and 3.1 mm respectively. The standard deviations are larger for the Y-model as compared to the X-model. This is expected due to an overall increase in motion. The 95% model has a standard deviation of 1.1 mm for both vectors. There is an increase for the 99% model to 1.3 mm, which is expected due to capturing an even broader range of motion. Figures 3.3 and 3.4 demonstrate the Polynomial model when applied to Y-vector data for two separate patients.

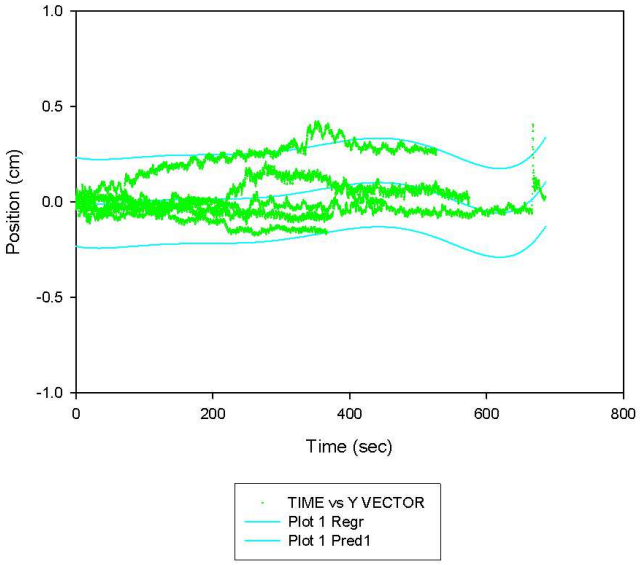

Figure 3.3 Polynomial fit for the X-model, CCF 125, 95% Predictive Line

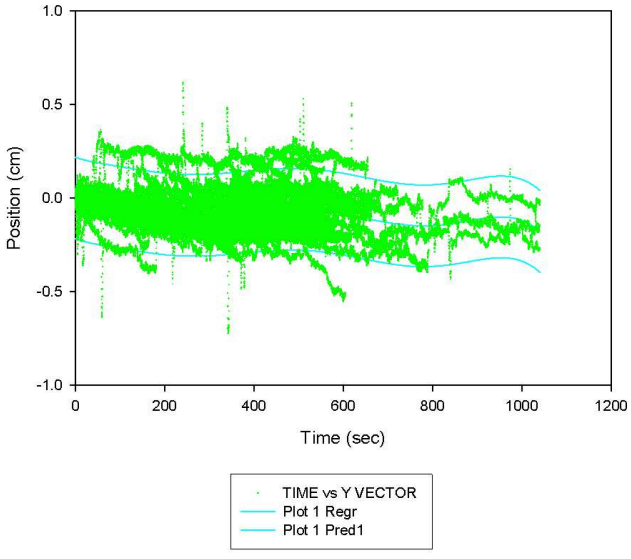

Figure 3.4 Polynomial fit for the Y-model, CCF 123, 95% Predictive Line

Figure 3.3 and 3.4 show more prostate motion than was demonstrated with the X-model. The spread in motion for patient CCF 125 is more pronounced when compared to the lateral motion. Although each treatment fraction begins at the initial coordinate of (0,0,0), the motion pattern varies for each fraction. This is in direct contrast to the previously presented X-model patients. This large motion expands the prediction line and results in larger predictive margins.

In the case of patient CCF 125, the predictive margins for the 95% model are 3.4 mm in the anterior direction and 2.9 mm in the posterior direction. Both of these margins are less than the 6/4 mm clinical model that is currently in use for IGRT patients. These margins also exceed the mean over the patient population, which indicates this patient has more motion than the other study patients. When the 99% prediction line is applied the margins are increased to 4.1 mm and 3.7 mm respectively. This is an increase and reduces the effectiveness in minimizing the volume of normal tissue being irradiated.

The results for CCF 123 are similar to CCF 125. The margins as defined by the 95% approach are 3.5 mm anterior and 2.7 mm posterior. This is similar to CCF 125. However, when the 99% criterion is applied, the margins for CCF 123 are 4.4 mm and 3.3 mm respectively. This indicates that there is more motion in CCF 123 when looking at the outlying data sets. Both of these patients exceed the mean margins. This is not indicative of all patients but underscores the need to be able to predict margins for patients on an individual basis. Table 3.4 shows the results of the margins as predicted using the Polynomial model in comparison with other clinical models.

Table 3.4 Summary of Comparisons between Accepted Clinical Models and the Polynomial Model for the Y-vector. Values indicate % of data points falling outside the clinical margins.

Patient	**2 mm**	**6/4 mm**	**Poly 95**	**Poly 99**
101	.25	0	.033	.012
102	5.5	.07	16.1	11
103	2.8	.07	.09	.011
106	7.7	.01	2	.91
108	.61	0	.04	0
109	8.9	.08	3.8	.77
110	8.7	.02	5.1	2
111	7.1	.03	2.7	1.3
112	.82	0	.05	0
113	.39	0	.64	.06
114	7.4	.78	7.9	5.1
115	16.9	.16	2.1	1
116	12.8	.22	4.3	2.1
117	14.4	.57	.64	.32
118	14.7	.04	7.5	4.7
119	4.5	.65	7.8	4.8
120	.31	0	.15	.026
123	14.4	.25	2.9	.84
124	10.6	.21	18.7	18.7
125	5.6	.3	1.6	1
126	7.1	.02	4.7	3.4
129	13.7	.28	17.8	6.3
130	6.6	.18	1.9	1.6
131	8.9	.24	15.6	11.4

A review of the clinical results from Table 3.4 show measurable differences among the models. The 2 mm model performed acceptably across all patients in the X-vector modeling process. However, the Y-vector introduces more physiological processes that increase this motion. For example, CCF 123 had 14.4% of the data points falling outside of the margin. A total of 7 patients performed unacceptably using the defined criteria for the 2 mm model.

The 6/4 mm model performs adequately. This is consistent with the concept that larger margins are effective in prostate therapy. All patients fell outside of the margins less than 1% of the time. This small value further supports the theory that uniform margins that are too large lead to an increase in dose to normal tissue while providing no additional benefit in dose to the prostate.

The Polynomial model results show significant differences from either of the two clinical models. The 2mm model performed unacceptably in over 29% of patients while the 6/4 mm model results show margins that are too large. Reviewing the 95% predictive model first shows a total of four patients falling into the unacceptable criteria. For example, CCF 124 had 18.4% of the data points fall outside of the clinical margins. This most likely indicates that the data accumulated over the first five fractions is not representative of the rest of the treatment fractions. The model predicted clinical margins of 1.5 mm in either direction. This value is the threshold set by the model below which treatment delivery cannot be delivered accurately.

The 99% approach shows an improvement. A total of three patients performed unacceptably based on the same criteria. CCF 129 had a reduction from 17.8% of the data points falling out of the margins to 6.3%when comparing 95% and 99% predictive line models. There are certain instances when moving from the 95%

model to the more encompassing 99% model is justified. Determining when this is necessary is not definitive and should be left to the clinician based on the individual patient. Overall the Polynomial model for the Y-vector performs satisfactory based on the results shown above. Using the 99% predictive line results in 85% of the patients scoring either adequate or marginal.

3.2.3 Polynomial, Z-model

The Z-vector represents motion in the superior / inferior directions. As is the case of the Y-vector, motion can be greatly influenced by physiological processes such as rectal gas and bladder fill rate. Given the nature of some of these processes, the motion pattern will exhibit various peaks throughout the treatment process. There is a possibility that motion found in the Z-vector will correlate with motion in the Y-vector. This correlation will be reviewed later in this chapter but should be noted. If these two models are related, there is a possibility of developing a model to predict motion in both models while looking at a combined set of data.

The results in Table 3.1 indicate the motion is very similar to the Y-vector. The mean for the 95% predictive approach is just less than 2.6 mm and the 99% model results in a mean value of less than 3 mm. These values represent motion in the superior direction. The inferior motion for the 95% and 99% models is 2.8 mm and 3.5 mm respectively. These mean values are almost identical with the Y data. This further confirms the potential for correlation between these components. The corresponding standard deviations are larger based on the overall increase in motion. The 95% model has standard deviations of 1 and 0.87. There is an increase for the 99% model, which is expected due to capturing an even broader range of motion. These values are 1.2 and .98 respectively. The standard deviations are slightly less for the Z-model, which can be attributed to the data being closer to the overall mean. Figures 3.5 and 3.6 represent the Z-model based on the 8^{th} order polynomial fit.

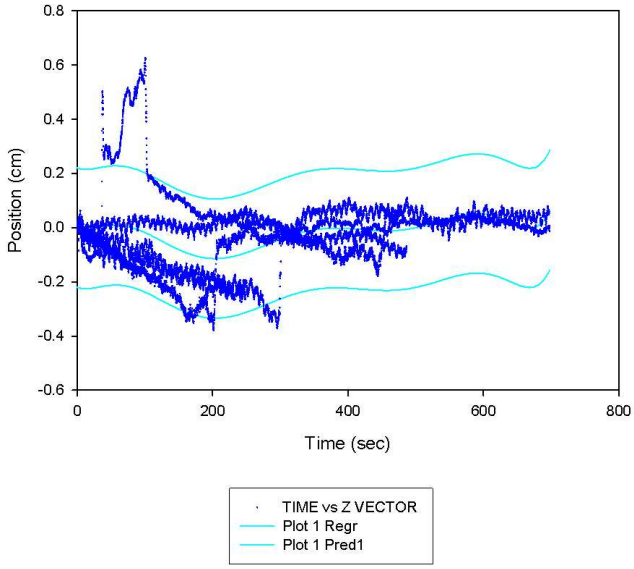

Figure 3.5 Polynomial fit for the Y-model, CCF 119, 95% Predictive Line

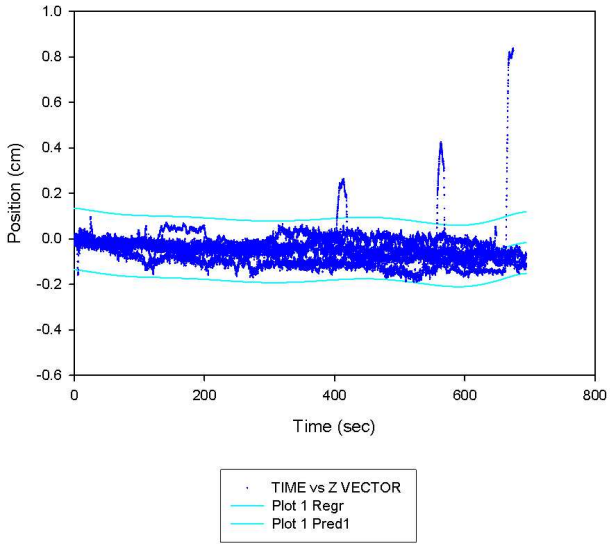

Figure 3.6 Polynomial fit for the Y-model, CCF 129, 95% Predictive Line

The figures above represent the polynomial model for the Z-vector. The 95% predictive lines are shown in these figures. CCF 119 shows significant motion variation over the first five fractions. This is accounted for in the model, which is evidenced by the motion of the predictive lines. There is a large motion deviation in the first 100 seconds for one fraction. This is more than likely attributed to rectal gas. This deviation is not seen in the other fractions that make up the clinical margins. The model needs to account for this since the largest point of inflection is used to determine the margin.

Patient CCF 129 is shows a pattern of motion that is limited. The margins are small relative to current clinical margins and may or may not be representative of the overall motion pattern for this patient. Table 3.5 summarizes the performance of the Polynomial approach for the Z-model across 24 patients.

Table 3.5 Summary of Comparisons between Accepted Clinical Models and the Polynomial Model for the Z-vector. Values indicate % of data points falling outside the clinical margins.

Patient	**2 mm**	**6/4 mm**	**Poly 95**	**Poly 99**
101	.24	.21	.21	.21
102	9	.02	7	2.3
103	4.3	.02	1.22	.97
106	15.1	.05	2.9	1.1
108	1.1	0	.84	0
109	6.1	.45	1.01	.76
110	13.3	2.4	7.3	4.4
111	6.6	.25	8.4	5.7
112	5.2	0	1.9	.074
113	.83	.01	.32	.32
114	9.6	.57	10.3	6.3
115	17.9	.03	2.8	.73
116	16.9	.12	1.5	.34
117	14.1	.69	1.92	1.1
118	8.6	0	2.3	.55
119	21.2	.09	4.6	3.4
120	.31	0	.21	0
123	7.2	.01	3.4	3.3
124	6	0	5.5	5.2
125	10.4	.55	3.7	2.8
126	8.2	.03	6.2	5
129	5.7	.02	3.4	3.2
130	2.4	.54	1.6	1.4
131	20.7	.3	21.1	13.3

The results shown above reflect the motion associated with the Z-vector. The 2 mm model does not perform satisfactory. A total of 8 patients had unacceptable results based on the criteria. This demonstrates that a uniform margin of 2 mm is not appropriate for clinical treatments. When reviewing the results of the 6/4 mm model, the results are as expected. The prostate moves outside of the treatment volume a small percentage of the time (< 1%). This confirms that the margins are too large across the patient population. All patients scored adequately with this approach.

The Polynomial model with the 95% prediction line performs satisfactory based on the results above. Only two patients perform unacceptably based on the criteria and one of the patients, CCF 114 misses passing by 0.3%. There are a larger number of patients falling within the marginal category. One of the figures above represented patient CCF 119. This patient scored in the adequate range. The second patient CCF 129 also performed in the acceptable criteria. This is important because the margins were relatively small (1.9 mm, 2.5 mm). Overall, the 95% prediction line model performed well over the 24 patients.

The Polynomial model utilizing the 99% prediction line also scored well. All patients show a decrease in the amount of data points falling outside the margins as expected. Only one patient had unacceptable results with this approach. CCF 131 did not perform well for the Y-model either. This appears to be a case of a bad sampling of data during the first five fractions. Both CCF 119 and CCF 129 saw decreases but not significant. Additional work will be needed in order to determine when an increase in margin is warranted based on the reduction in points outside of the field. With 23 of the 24 patients performing either acceptable or marginal, the Polynomial approach on the Z-vector is a valid method in predicting prostate treatment margins.

3.1.4 Summary of Polynomial Model Results

A total of 24 patients have been modeled using the Polynomial approach. The model was further broken down into two separate methods. One model used a 95% predictive line to determine clinical margins while the second approach used a 99% predictive line. Both approaches were attempted in order to determine which model would provide better margins.

The X-model has been consistent across all of the patients presented and that consistency is present in most all of the patients presented. In addition, there is very little difference whether the clinician chooses the 95% or the 99% prediction line for margins. However, it should be noted that due to the overall lack of motion in the X-vector, the model threshold was utilized in over 70% of the patients. In this research, a total of 14 of the 24 patients (95% Polynomial) were assigned the 1.5 mm margins. The other 10 patients showed minimal increases in margins. These results indicate that margins are predictable and a uniform approach across the entire population can be assumed for the X-model.

Unlike the X-model, the Y-model experienced more motion over the course of 24 patients. This is not unexpected in that the bladder fill along with rectal gas would have a significant influence on the pattern of motion. The Polynomial model performed well under these conditions. A total of 16 patients in the 95% model and 19 patients in the 99% model performed acceptably. This is lower than the X-model but not unexpected given the factors that affect motion in the anterior / posterior directions. The main concern with the results is the subset of patients that performed unacceptably with greater than 10% falling outside the range. This was reduced with the 99% model. Even with several patients outside of the 10% range, 87.5% of the patients scored acceptable or marginal. The 8^{th} order Polynomial fit is successful in predicting prostate motion for the Y-model in most of the patients. .

The results of the Z-model are similar to the results presented regarding the Y-model. Although no correlation between the two movements has been shown, there appears to be a qualitative relationship between the vectors on several patients. The results for the Z-model are consistent with the Y-model in the number of patients who perform acceptably under the criteria. The Z-model actually performs better from the standpoint of having less patients fall into the unacceptable category. An increase occurs in the marginal range in both the 95% and the 99% models. The Z-model performs well across all patients. Over 90% of the patients scored in the acceptable or marginal range with either model.

Overall, the Polynomial model is effective in predicting clinical treatment margins and reducing the overall volume of normal tissue that will be irradiated. There are several patients where the model does not accurately model motion. In these cases, it will be necessary to look at ways in order to minimize this from happening in future cases. In addition, due to a lack of motion in the lateral direction, a uniform model across all patients appears to be satisfactory for the general patient population.

3.2 Cumulative Frequency Distribution Model (CFD)

In order to determine the effectiveness of the Polynomial model, a different statistical approach was researched. The CFD was determined to be an acceptable approach at modeling the prostate motion. One advantage to this model is that it is very simple to apply. A ranking of the data allows the user to determine the 95% and 99% points in the set. Another benefit is that this is using the actual patient data so the effects of a model are not present. This has the potential to reduce the influence of distributions that are not accurate or may skew the results. Tables 3.6 and 3.7 summarize the results for the CFD approach using the 95% and 99% data points

Table 3.6 Clinical margins (in millimeters) for the CFD model utilizing the 95% data point.

Patient	**+X**	**-X**	**+Y**	**-Y**	**+Z**	**-Z**
101	1.5	1.5	1.8	1.5	2.6	1.5
102	1.5	2.8	1.5	1.5	1.5	2.2
103	1.5	1.5	3.3	1.8	2.3	1.7
106	1.5	1.5	1.5	2.4	1.5	2.5
108	1.5	1.5	3.8	1.9	2.9	1.5
109	1.5	1.5	1.7	1.5	2.8	1.7
110	1.5	1.5	2.6	1.5	1.7	1.5
111	1.5	1.5	1.5	2.3	1.5	1.5
112	1.5	1.5	2.3	1.5	3	1.5
113	1.5	1.5	1.5	1.5	1.5	1.5
114	1.5	1.5	2.5	1.5	2.1	1.5
115	1.5	1.5	1.5	2.3	1.5	2.9
116	1.5	1.5	1.5	1.5	2.1	1.5
117	1.5	1.5	6.8	2.7	4	2.1
118	1.5	1.5	1.5	2.2	1.5	2.6
119	1.5	1.5	1.5	1.5	1.5	2.4
120	1.5	1.5	1.7	1.5	1.9	1.6
123	1.6	1.5	2	1.8	1.5	2.1
124	1.5	1.5	1.5	1.5	1.5	1.5
125	1.5	1.5	2.9	1.5	2.8	1.5
126	1.5	1.5	1.5	1.9	1.5	1.8
129	1.5	1.5	1.5	1.5	1.5	1.5
130	1.5	1.5	1.5	1.5	1.5	1.5
131	1.5	1.5	1.6	1.5	1.5	1.5
Mean	1.50	1.55	2.12	1.74	1.99	1.79
S Dev.	0.02	0.26	1.19	0.37	0.69	0.43

Table 3.7 Clinical margins (in millimeters) for the CFD model utilizing the 99% data point.

Patient	**+X**	**-X**	**+Y**	**-Y**	**+Z**	**-Z**
101	1.5	1.5	2.7	2.6	4.2	2.8
102	1.5	2.8	1.5	1.5	1.5	2.4
103	1.5	2	4.7	3.2	3.3	3.6
106	1.5	1.5	1.5	3.6	1.2	2.9
108	1.5	2	4.2	1.8	3.3	1.5
109	1.5	1.5	4.9	1.9	6.2	2.5
110	1.6	1.5	3	1.5	4.5	1.9
111	1.5	1.5	1.5	3.1	1.5	1.8
112	1.5	1.5	3	1.5	5.5	2.4
113	1.5	1.5	1.5	1.5	1.5	1.5
114	1.5	1.5	3.2	1.5	3.6	1.5
115	1.5	1.5	1.5	3.4	1.5	3.6
116	1.6	1.5	2.9	1.5	4.9	2
117	1.5	1.5	8.5	5.1	6.8	3.9
118	1.5	1.5	1.5	2.9	1.5	2.9
119	1.5	1.6	1.5	1.7	4.8	3.2
120	1.5	1.5	3.4	1.5	5.6	2.7
123	1.9	1.5	2.4	2.2	1.5	2.4
124	1.5	1.5	1.5	1.5	1.5	1.7
125	1.5	1.5	3.7	1.6	3.7	1.5
126	1.5	1.5	2.2	1.5	2.2	1.5
129	1.5	1.5	1.5	3.6	1.5	2
130	1.5	1.5	1.5	2.1	2.1	5.2
131	1.5	1.5	1.6	2.1	1.8	2
Mean	1.52	1.6	2.72	2.27	3.15	2.47
S Dev.	0.08	0.29	1.65	0.96	1.78	0.93

The CFD approach is simplified statistical method that does not require complex equations or functions in order to generate predictive margins. In order to determine its effectiveness when compared to other clinical models, the results will be divided into sections that discuss each vector component separately. In addition, this will be effective in comparing results that were obtained with the Polynomial approach.

3.2.1 CFD, X-model

The results for the X-model using the CFD approach are summarized in the Tables 3.6 and 3.7 above. Analysis of the 95% data point model show that the lateral margins are smaller than what was seen the Polynomial approach. The means are 1.5 and 1.6 respectively. This is not a significant difference but it does show that the majority of the margins were assigned the threshold value of 1.5 mm in either direction. The standard deviation is .02 and .26 mm. This confirms that there is a lack of variation from the mean which suggests minimal data motion over the patient population. This is consistent with the Polynomial model.

The results of the 99% data point analysis are very similar. The means are reported as 1.5 and 1.6 respectively. The motion detected in the negative lateral direction has only a slight difference in the mean between the 95% and 99% models. If there is not a significant increase in margins between approaches it confirms that the data is limited in motion. When the prostate demonstrates limited displacement, a uniform approach is supported. The benefit to a uniform model is that margins can be generalized over a patient population. This is the case in the clinical models that are analyzed when comparing the predictive margin approaches (2 mm and 6/4 mm). The issue is that the margins being suggested are small and based on the minimum size necessary in order to deliver an accurate treatment. Another size margin might be more appropriate for the general population. That is one of the questions to be answered in future research. Figures 3.7 and 3.8 represent the X-model for the CFD approach.

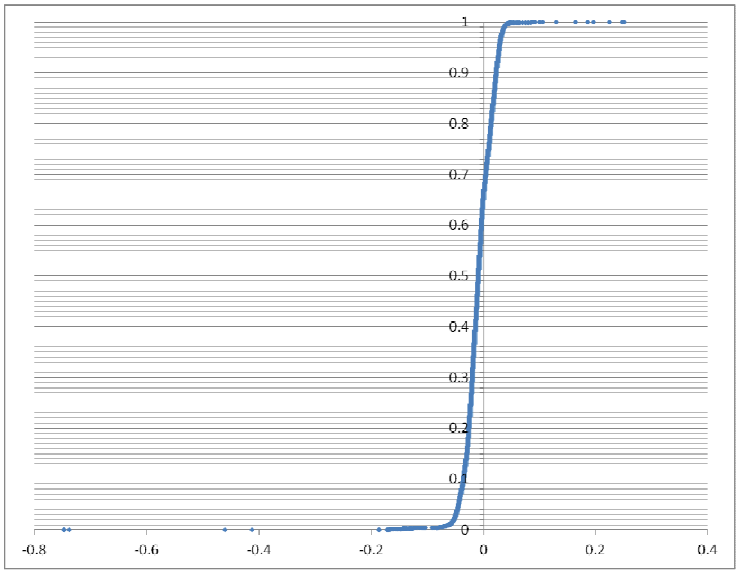

Figure 3.7 CFD for Patient CCF 101, X-model

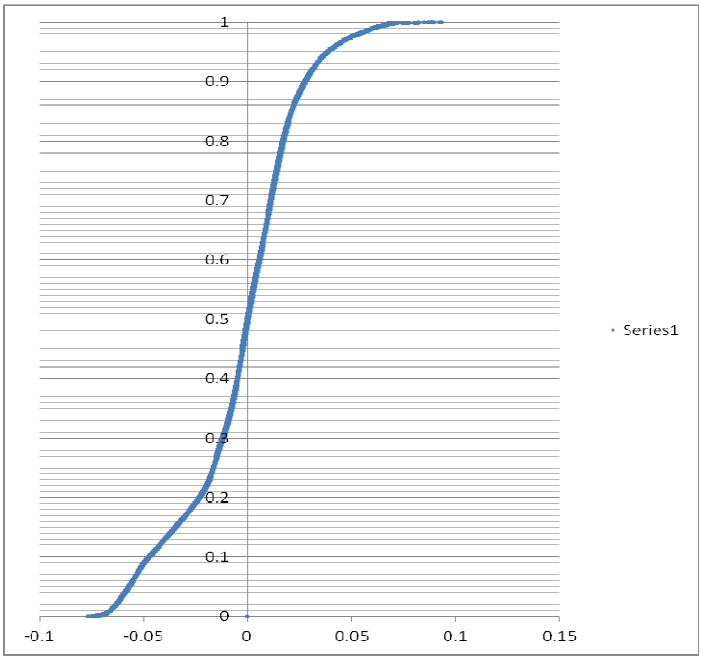

Figure 3.8 CFD for Patient CCF 115, X-model

The first figure represents patient CCF 101. As previously shown in the Polynomial model, there is minimal motion (< 2 mm) in the lateral directions. The margins summarized in Tables 3.6 and 3.7 demonstrate that the CFD supports that result. Figure 3.7 displays a uniform displacement around the zero point over the first five fractions. This results in very small margins in comparison to current clinical models. The predicted margins are 1.5 mm which is the threhold for treatment delivery established in this research. The CFD approach is consistent with the Polynomial model. When there is limited motion, the model will predict tight margins with either approach.

Patient CCF 115 has less motion than the previous patient. This again is supported by the Polynomial approach. The motion pattern does not exceed 1 mm across all five fractions. The 1.5 mm threshold will be used in setting the margins for this particular patient. The 1.5 mm margin is consistent throughout the CFD approach. The mean is close to 1.5 in either direction and model. The Polynomial approach has a mean of 1.6 and 1.8 across the 99% model. The results indicate that the CFD approach predicts narrow margins across the patient population for the X-model in comparison to the Polynomial model. This would make the model more effective if it results in a reduction of data points falling outside of the margins when compared to other clinical models.

Given the overall lack of motion in the lateral direction of the prostate, the model assumes the threshold margins in over 95% of the patients. This is higher than in the Polynomial model. The comparison of the CFD model with the two other clinical models is shown in Table 3.8.

Table 3.8 Summary of Comparisons between Accepted Clinical Models and the CFD Model for the X-vector. Values indicate % of data points falling outside the clinical margins.

Patient	**2 model**	**6/4 mm**	**CFD 95**	**CFD 99**
101	.015	0	.024	.024
102	5.91	0	1.8	1.8
103	0	0	.16	.16
106	2.1	0	3.3	3.3
108	.02	0	.96	.022
109	.05	0	1.9	1.9
110	1.24	0	3.4	3.4
111	.42	.04	1.3	1.3
112	.68	0	1.8	1.8
113	0	0	0	0
114	.02	0	.023	.023
115	0	0	0	0
116	3.4	0	11.7	10.8
117	2.8	0	7.2	7.2
118	3.4	0	3.5	3.5
119	2.8	0	9.7	7.9
120	0	0	0	0
123	2.8	0	4.2	2.2
124	.23	.07	1.2	1.2
125	.75	0	2.6	2.6
126	3.7	0	3.1	3.1
129	0	0	0	0
130	.04	0	2.4	2.4
131	.16	0	1.4	1.4

The results shown in Table 3.8 summarize the performance of predictive margins as determined using the CFD approach. The results show that the model performs adequately for 21 of the 24 patients when using the 95% criteria. Only one patient had an inadequate result based on the established criteria. When compared with the other clinical models, the 95% model is equivalent in delivering dose within acceptable treatment margins. The 2 mm model has similar results. The 6/4 mm model results demonstrate that there is little gain in accuracy for the increase in margins and dose to normal tissue.

When reviewing the 99% model, there is very little change in margins or results. There is a minimal reduction in the number of data points falling outside of the margins. This is confirmed by reviewing the mean margins. Due to the minimal motion in the prostate in the lateral directions, there is no gain in applying the 99% model for patients. Patient CCF 116 was inadequate with a value of 11.7% in the 95% approach and improved only slightly to 10.8% when using the 99% criteria.

The results with the CFD model are similar to the Polynomial model for the X-vector. Over 90% of the patients perform adequately under the set criteria. The limited motion of the prostate as demonstrated by both models is consistent with a uniform margin approach.

3.2.2 CFD, Y-model

The Y-vector has more motion due to physiological proccesses than the X-vector. The reasons for this have been previously discussed. The Polynomial approach for the Y-vector resulted in over 90% of the patients scoring an adequate or marginal result. Figures 3.9 and 3.10 show the CFD model for the Y-vector.

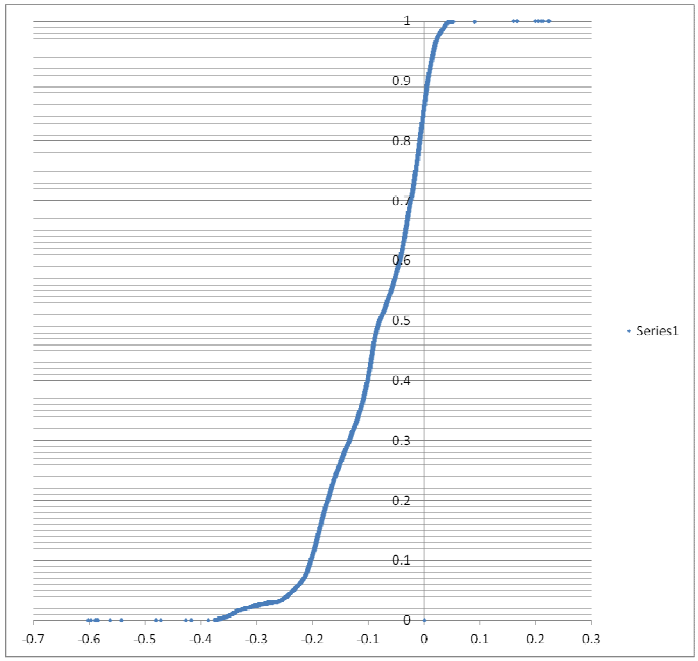

Figure 3.9 CFD for Patient CCF 115, Y-model

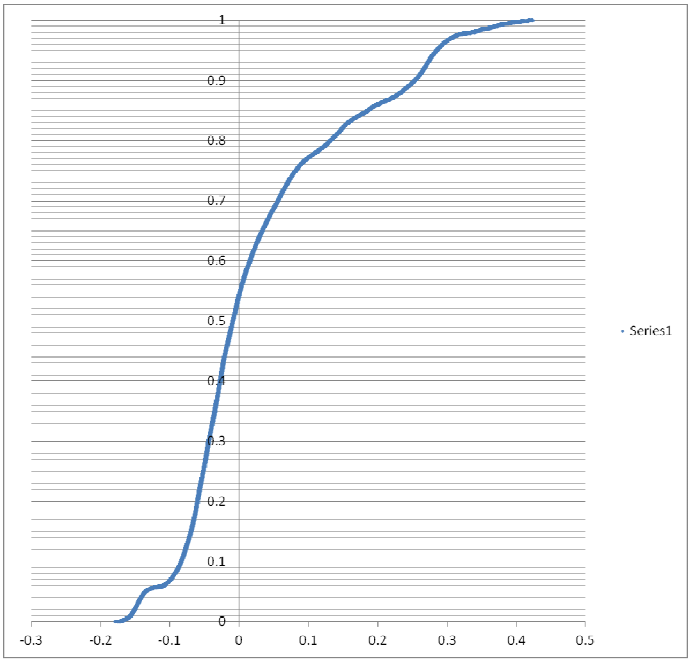

Figure 3.10 CFD for Patient CCF 125, Y-model

A review patient CCF 115 shows more motion in the Y-vector. This motion is anticipated based on the results shown earlier. The CFD approach is effective in showing where the majority of the motion occurs. In the case of CCF 115, the motion is skewed in the posterior directions over all five fractions. This leads to larger margins for the posterior edge of the prostate gland. The corresponding margins for the 95% approach are 1.5 mm in anterior direction and 2.3 mm in the posterior. The model does note the posterior motion of the gland. The CFD model is able to predict margins outside of the model threshold for this patient. The Polynomial model was more effective in modeling this movement and extending the posterior margin. When reviewing the 99% approach, the same issue can be noted with regards to posterior motion. The model predicted a 3.4 mm margin. This increase is an improvement but still below the 3.8 mm predicted with the Polynomial model.

Patient CCF 110 presents with the opposite motion pattern. Prostate displacement occurs in the anterior direction over the first five fractions. The CFD approach models this motion by extending margins in the anterior direction to 2.6 mm in the 95% and 3 mm in the 99% models. There are more data points at extended distances from the isocenter which the model is able to incorporate in its prediction. These margins are still significantly smaller than the Polynomial model. The Polynomial approach predicts 3 mm at the 95% and 3.5 mm at the 99% data point.

The CFD model predicts smaller margins when compared to the Polynomial model across the patient population in this research. This is effective if it results in the same outcome as seen the Polynomial model. The summary of the Y-model using the CFD approach in comparison to other clinical models is given in Table 3.9.

Table 3.9 Summary of Comparisons between Accepted Clinical Models and the CFD Model for the Y-vector. Values indicate % of data points falling outside the clinical margins.

Patient	**2 mm**	**6/4 mm**	**CFD 95**	**CFD 99**
101	.25	0	1.9	.037
102	5.5	.07	16.1	16.1
103	2.8	.07	1.8	.097
106	7.7	.01	7.2	4.1
108	.61	0	.08	0
109	8.9	.08	14.2	4
110	8.7	.02	7.4	6
111	7.1	.03	5.6	3.7
112	.82	0	.42	.21
113	.39	0	.64	.64
114	7.4	.78	10.5	9.8
115	16.9	.16	11.5	2.4
116	12.8	.22	22.1	18.5
117	14.4	.57	.74	.28
118	14.7	.04	12.2	5.8
119	4.5	.65	11.7	9.1
120	.31	0	1.1	.075
123	14.4	.25	19.3	8.6
124	10.6	.21	18.7	18.7
125	5.6	.3	7.4	5.7
126	7.1	.02	9.9	9.6
129	13.7	.28	28.4	12.5
130	6.6	.18	12.8	12.5
131	8.9	.24	16.4	13.1

The summary of the results in Table 3.9 show a model that does not perform well in predicting treatment margins. A total of 50% of the patients had inadequate results when using the 95% criteria. This is up substantially from the Polynomial model. The number of data points falling outside the margins is reduced to 29% when using the 99% criteria. These results demonstrate that the CFD does not perform adequately across the population.

The 2 mm model underperforms as well. A total of 29% of the patients had an inadequate result using this approach. A uniform 2 mm margin approach does not appear to be an acceptable approach in applying margins to prostate motion for the Y-vector. As expected, the 6/4 mm model showed the effect of over margining. None of the patients exceeded the margins more than 1% of the time.

The CFD approach is not recommended for predictive margins when reviewing the results of the Y-model. The model consistently underestimates the necessary margins for accurate motion management. This is even more pronounced when compared to the Polynomial model. The CFD model will be analyzed when applied to the Z-vector data in the next section.

3.2.3 CFD, Z-model

The Z-vector has a similar motion pattern to the Y-vector. The Polynomial approach resulted in over 95% of the patients scoring an adequate or marginal result when using the 99% criteria for the Z-model. Figures 3.11 and 3.12 show the CFD model for the Z-vector.

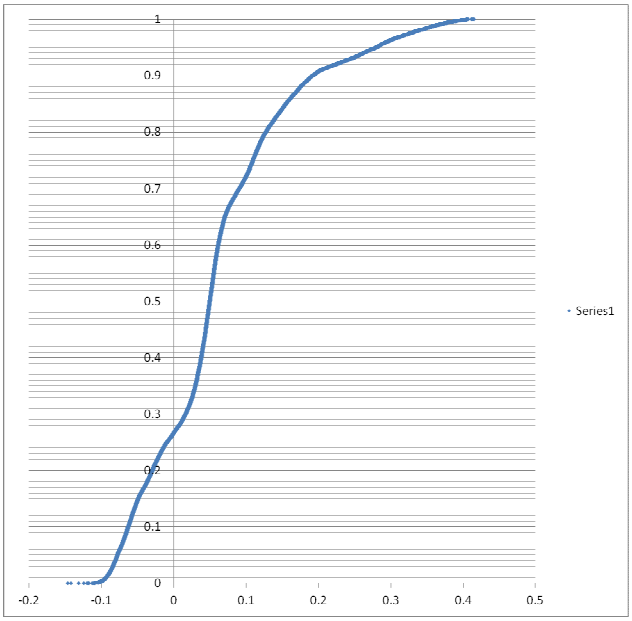

Figure 3.11 CFD for Patient CCF 125, Z-model

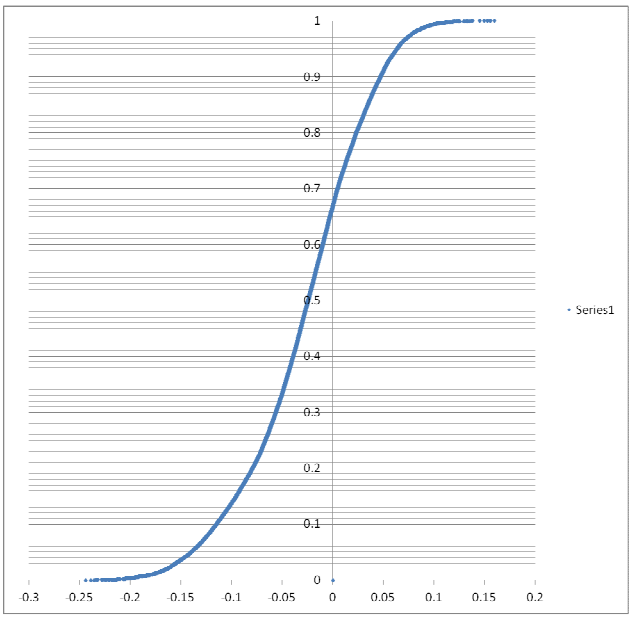

Figure 3.12 CFD for Patient CCF 111, Z-model

The review of the Z-model for the CCF 125 shows the majority of motion is in the superior direction. There is minimal motion (< 2 mm) in the inferior direction. The lack of motion in the inferior direction will result in a margin of 1.5 mm being assigned in both the 95% and 99% approaches. This is in contrast to the Polynomial model where the inferior margins were estimated in the range of 2.4 for the 95% and 2.6 mm for the 99% given the same dataset. The 95% approach predicts a margin of 2.8 mm in the superior direction while the Polynomial model predicts 3.1 mm. The estimates from both approaches are different, especially along the superior border.

Patient CCF 111 shows a more uniform motion pattern with minimal motion (< 2mm) along the superior border. This is in direct contrast to patient CCF 125. The result of this motion pattern is that the predicted margins for the 95% model are 1.5 mm in either direction. The Polynomial model estimated margins to be 1.5 and 1.9 mm. With minimal displacement, either approach estimates small margins. The 99% criteria estimates margins of 1.5 mm superiorly and 1.9 mm inferiorly. This is minimal gain in the inferior direction but consistent with the Polynomial model.

The results of the two patients above show that the CFD model in these instances predicts small margins with respect to current clinical models. The model threshold is assigned in 54% of the patients. Given the results previously presented with the Polynomial model, it is not probable that these predictive margins will satisfy the acceptance criteria set forth for this research. Table 3.10 gives the results for the CFD model when applied across all 24 patients for both the 95% and 99% criteria.

Table 3.10 Summary of Comparisons between Accepted Clinical Models and the CFD Model for the Z-vector. Values indicate % of data points falling outside the clinical margins.

Patient	**2 mm**	**6/4 mm**	**CFD 95**	**CFD 99**
101	.24	.21	.21	.21
102	9	.02	6.9	4.8
103	4.3	.02	6.4	.56
106	15.1	.05	9.3	6.3
108	1.1	0	1.9	1.7
109	6.1	.45	6.6	1.8
110	13.3	2.4	21.2	5.5
111	6.6	.25	15.6	5.1
112	5.2	0	5.6	2.8
113	.83	.01	3.2	3.2
114	9.6	.57	15.3	14.2
115	17.9	.03	4.4	2.6
116	16.9	.12	29.2	12.1
117	14.1	.69	8.4	1.4
118	8.6	0	4.4	3
119	21.2	.09	33.8	1.8
120	.31	0	.61	0
123	7.2	.01	7.3	4.2
124	6	0	7.3	6.8
125	10.4	.55	5.2	3.5
126	8.2	.03	8	6.5
129	5.7	.02	14.4	13.3
130	2.4	.54	8.3	1.6
131	20.7	.3	34.6	24.2

A review of results in Table 3.10, demonstrates that the CFD model using the 95% criteria is not suitable in modeling the Z-vector. A total of 29% of the patients performed inadequately using the established criteria. The patients in this category had larger misses when compared to the Polynomial model. For example, CCF 131 had 34.6 percent of the data points fall outside of the margins. CCF 119 had a total of 33.8% as well. Misses of this size indicate that the model is not suitable for predictive margins. Another issue is the increase in the number of patients scoring marginally. A total of 45.8% of the patients had marginal results. This is in contrast to the Polynomial model which had 20.8% of the patients score marginally. The performance of the CFD model using the 95% criteria is well below the Polynomial.

There is improvement in the model when using the 99% criteria. A total of 16.7% of the patients have inadequate results when using the same criteria. The most significant improvement is seen in CCF 119. The 95% model has 33.8% falling outside the margins while the 99% has only 1.8%. This reduction indicates that the majority of the motion was just outside of the margins determined in the 95% approach. These results are still less than those obtained with the Polynomial model. The increase in margins when comparing the CFD 95% versus CFD 99% is not significant. This is most likely related to the use of the actual data as opposed to a modeling approach such as the Polynomial.

The CFD for the Z-model does not perform as well as the Polynomial model. It consistently under predicts margins and leads to large amounts of data points falling outside of the treatment margins. A summary of the performance of the CFD approach is given in the next section.

3.2.4 Summary of CFD Model Results

The CFD is a simplified statistical approach that was attempted in order to determine the best method to model prostate motion. A Polynomial model has been developed that performed satisfactory across 24 patients. The CFD model has been applied to those same patients. The reasoning behind the CFD approach is that it utilizes actual data points for modeling and it is a statistical method that can be easily implemented. The criteria for determining the success of a model is given in Table 2.1. Once the data is ranked, the 95% and 99% data points are determined and used as the clinical margins. These are then compared with other clinical models to determine effectiveness of the model.

Results of the CFD approach with respect to the X-model are very similar to the Polynomial model. The X-model scored well using the CFD approach. The main reason behind this is that there is very little motion in the lateral directions of the prostate and that the model threshold of 1.5 mm is assigned in a number of the patients. This is important since margins that are too small cannot be delivered due to uncertainties such as setup error and patient positioning. The performance of the CFD for the X-model is summarized in Table 3.8.

The Y-model has more motion when compared to the X-vector as seen in the results of the Polynomial approach. The results for the Y-model using the CFD are given in Table 3.9. The results for the Y-model across the population are poor. Approximately 54% of the patients were inadequate using the 95% criteria. This is up from 20.8% using the Polynomial approach. With only six patients scoring in the adequate range and 5 in the marginal range, the 95% model is not suitable for clinical delivery. The 99% approach is improved with approximately 29% of the patients not meeting the criteria for either adequate or marginal performance. These results are significantly higher than the Polynomial model and represent an

underperforming model. The Y-model is ineffective at predicting motion regardless of which approach (i.e. 95% or 99%) is chosen.

The results for the Z-model are mixed. There is improvement from the Y-model across all criteria. However, the adequate criterion is only met by 25% of the patients using the 95% approach. This is not clinically acceptable. There is slight improvement in the 99% model (58% are adequate) but not enough to consider this as an alternative to the Polynomial model. A total of 7 and 5 patients respectively had inadequate results in the 95% and 99% approaches. This is above the Polynomial model. The CFD model does not model motion that results in large displacements of the prostate.

3.3 The Bayesian Model

The initial approach to modeling prostate motion centered on the Polynomial model. This model was found to be suitable across a population of 24 patients. In order to validate this approach, a more straightforward statistical method was attempted. The CFD model was then applied to the same 24 patients. The results were mixed and overall, the model underperformed across a majority of the patients. The third and final method attempted is the Bayesian model. The theory behind this statistical model has been presented in Chapter 2.

One advantage of the Bayesian method is that it uses the likelihood as a function to predict motion. The likelihood function is determined by using a model that accurately fits the data. In this case, a Gaussian model was chosen based on research (Khan, 2008). The predictive margins as determined by the Bayesian approach are provided in Tables 3.8 and 3.9 below.

Table 3.11 Clinical margins (in millimeters) for the Bayesian model utilizing the 95% data point.

Patient	**+X**	**-X**	**+Y**	**-Y**	**+Z**	**-Z**
101	1.5	1.5	1.7	1.6	2.1	1.7
102	1.5	2.7	1.5	1.5	1.6	2.3
103	1.6	1.5	3.8	3	2.7	2.9
106	2	2.1	1.7	3	2.1	3.4
108	1.9	2.1	3.8	2.9	3.5	2.1
109	1.5	1.5	2.9	2.3	3.6	3.5
110	1.5	1.5	3	1.5	2.6	2.1
111	1.5	1.5	1.5	3	1.5	1.8
112	1.5	1.5	2.5	2.3	4.2	3
113	1.5	1.5	2.4	2	2.4	2
114	1.5	1.5	2.3	2	2.4	2
115	1.5	1.5	2.3	2	2.4	2
116	1.5	1.5	2.1	2.3	3.3	3.8
117	1.5	1.5	5.4	5.7	3.8	4.2
118	1.5	1.5	1.5	2.6	1.5	3
119	1.5	1.5	1.5	2.6	1.5	3.1
120	1.5	1.5	2.4	1.8	2.9	3.2
123	2.2	2.2	2.7	2.9	1.5	2.6
124	1.5	1.5	1.5	1.5	1.5	2.1
125	1.5	1.5	3.3	2.7	3.1	1.9
126	1.5	1.5	1.5	2.3	1.5	2
129	1.5	1.5	2	2.6	1.5	2.2
130	1.5	1.5	2.2	2.5	1.5	2.2
131	1.5	1.5	1.9	1.5	2.4	1.8
Mean	1.57	1.63	2.39	2.42	2.37	2.54
St. Dev	0.18	0.31	0.95	0.87	0.85	0.71

Table 3.12 Clinical margins (in millimeters) for the Bayesian model utilizing the 99% data point.

Patient	**+X**	**-X**	**+Y**	**-Y**	**+Z**	**-Z**
101	1.5	1.5	2.1	2.1	2.4	2.1
102	1.5	3.7	1.5	1.9	2	2.8
103	2	1.6	4.6	3.8	3.4	3.6
106	2.5	2.6	2.2	3.6	2.7	4
108	2.3	2.6	4.5	3.7	4.2	2.8
109	1.5	1.5	3.5	2.9	4.5	4.3
110	1.6	1.8	3.5	1.8	3.2	2.7
111	1.5	1.5	2	3.5	1.6	2.1
112	1.5	1.5	3	2.8	5	3.8
113	1.8	1.5	2.8	2.5	2.9	2.5
114	1.5	1.5	2.8	2.5	2.9	2.5
115	1.5	1.5	2.8	2.5	2.9	2.5
116	1.8	1.5	2.6	2.8	4.2	4.6
117	1.5	1.5	6.8	6.9	4.8	5.2
118	1.5	1.5	1.5	3	1.9	3.5
119	1.5	1.5	1.5	3	1.8	3.6
120	1.5	1.5	2.9	2.3	3.6	4
123	2.7	2.7	3.3	3.6	1.5	3
124	1.5	1.5	1.5	1.5	1.5	2.4
125	1.5	1.5	4	3.4	3.7	2.4
126	1.5	1.9	1.5	2.7	1.7	2.4
129	1.5	1.5	2.6	3.1	1.7	2.6
130	1.5	1.5	2.8	3.1	1.7	2.6
131	1.5	1.7	2.3	1.7	2.9	2.3
Mean	1.67	1.77	2.86	2.94	2.86	3.09
St. Dev	0.35	0.56	1.23	1.07	1.11	0.86

A total of 24 patients have been analyzed using three different statistical methods. The first two approaches centered on the Polynomial model and the Cumulative Frequency Distribution. The Bayesian model is the final approach attempted. Using a function that fits the data, a model is developed using the 95% and 99% data points. Each vector model is presented in detail in the following sections.

3.3.1 Bayesian, X-model

The results for the X-model using the Bayesian approach are summarized in the Tables 3.8 and 3.9 above. Analysis of the 95% data point model shows that the lateral margins are larger than was seen with the CFD approach but almost identical with the Polynomial model. The mean is 1.6 mm and 1.6 mm respectively. The lack of difference between all three models is indicative that the lateral motion of the prostate is best modeled using a uniform margin approach. The standard deviation is .03 and .1 mm with the Bayesian model. This confirms that there is a lack of variation from across the population.

The results of the 99% data point analysis are similar. The mean is reported as 1.7 mm and 1.8 mm respectively. There is an increase in margins in both lateral directions but not by a significant amount. If there is not a significant increase in margins between approaches it confirms that the data has limited motion. The results with the Bayesian approach are similar to the previous results presented for both models. The standard deviation for the 99% data point approach is .35 and .31. This increase is not unexpected based on the model approach. Figures 3.13 and 3.14 represent the X-model for the Bayesian approach.

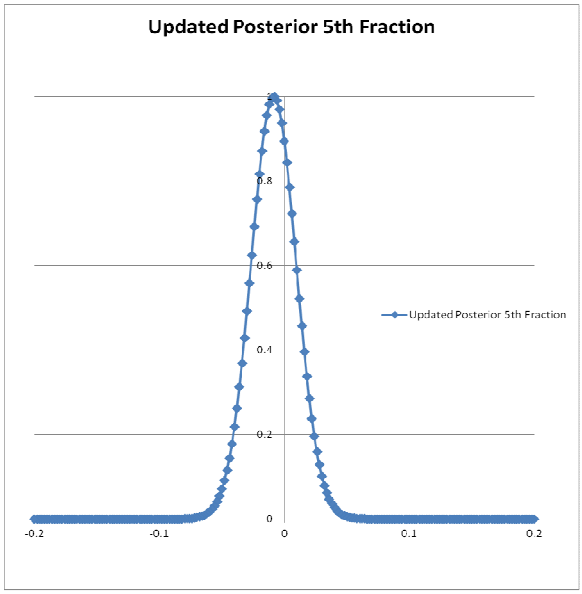

Figure 3.13 Posterior Distribution for Patient CCF 101, X-model

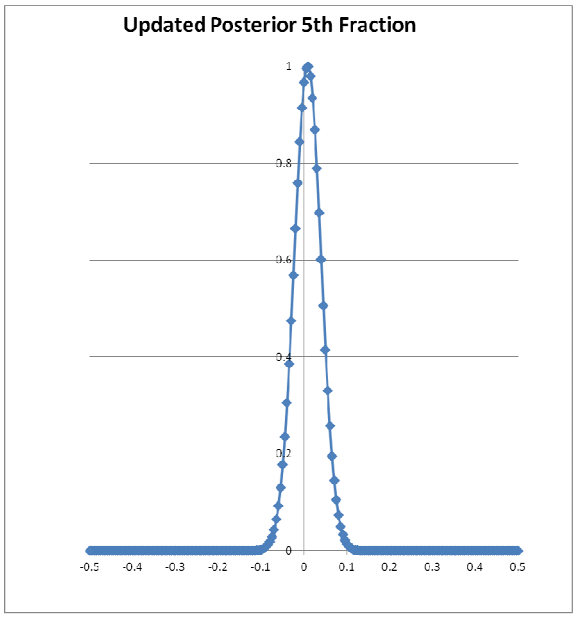

Figure 3.14 Posterior Distribution for Patient CCF 131, X-model

The Bayesian model for CCF 101 demonstrates limited motion over the first five fractions. The distribution is nearly centered in along the zero point. This shows a uniform motion pattern. The predictive margins fall below the threshold of 1.5 mm as set in this research. This result is seen in the other models as well. There is no change in margin whether the 95% or the 99% points are used.

The second patient shown is CCF 131. The posterior distribution shows a skew to the postive lateral margin during the first five fractions. This is similar with CCF 101 in that the predictive margins will be 1.5 mm as well. The margins do not change whether choosing the 95% or 99% points.

The posterior distribution shows similar results with the Polynomial and CFD models. The mean and standard deviation across all three models are not signficnatly different. The results of the Bayesian model are consistent with previous modeling methods. The results of the Bayesian model applied across all patients is shown below in Table 3.10.

Table 3.13 Summary of Comparisons between Accepted Clinical Models and the Bayesian Model for the X-vector. Values indicate % of data points falling outside the clinical margins.

Patient	2 mm	6/4 mm	Bayes 95	Bayes 99
101	.015	0	.024	.02
102	5.91	0	2.1	.54
103	0	0	.16	.01
106	2.1	0	2.1	2.1
108	.02	0	.01	.01
109	.05	0	1.9	1.9
110	1.24	0	3.4	3.2
111	.42	.04	1.3	1.3
112	.68	0	1.8	1.8
113	0	0	0	0
114	.02	0	.02	.02
115	0	0	0	0
116	3.4	0	11.7	8.5
117	2.8	0	7.2	7.2
118	3.4	0	3.5	3.5
119	2.8	0	9.7	9.7
120	0	0	0	0
123	2.8	0	2.7	2.1
124	.23	.07	1.2	1.2
125	.75	0	2.6	2.6
126	3.7	0	3.1	2.9
129	0	0	0	0
130	.04	0	2.4	2.4
131	.16	0	1.4	1.4

The results of the clinical comparisons show strong similarities with the Polynomial and CFD approaches. There is very little difference between the 95% and 99% models. The consistency demonstrates a uniform margin approach will be effective in managing prostate motion for patients.

A review of the 95% data shows that only one patient was unacceptable. CCF 116 had 11.7% of the data fall outside of the treatment margins. That is the same for the CFD model but higher than the 8.5% measured with the Polynomial method. However, when the 99% criterion is applied, CCF 116 falls into the marginal category with only 8.5% falling outside of the margins.

A review of the 99% model shows that no patients are unacceptable with respect to the established criteria. The Bayesian model outperforms the CFD. In comparison to the Polynomial model, there is very little difference. Several patients have a slightly higher rate of data points falling outside the margins but the Bayesian approach has slightly smaller margins averaged over 24 patients versus the Polynomial model when using the 95% data.

3.3.2 Bayesian, Y-model

The Y-model shows significantly more motion (> 2 mm) than seen in the X-model. The Polynomial model had over 90% of the patients score as acceptable, while the CFD approach had only 50% rate as score in the acceptable range with the 95% model. Since the majority of patients motion is Gaussian in nature (Khan, 2008), the Bayesian model should be effective in estimating motion. Figures 3.15 and 3.16 represent the Posterior distribution for two of the 24 patients presented for review.

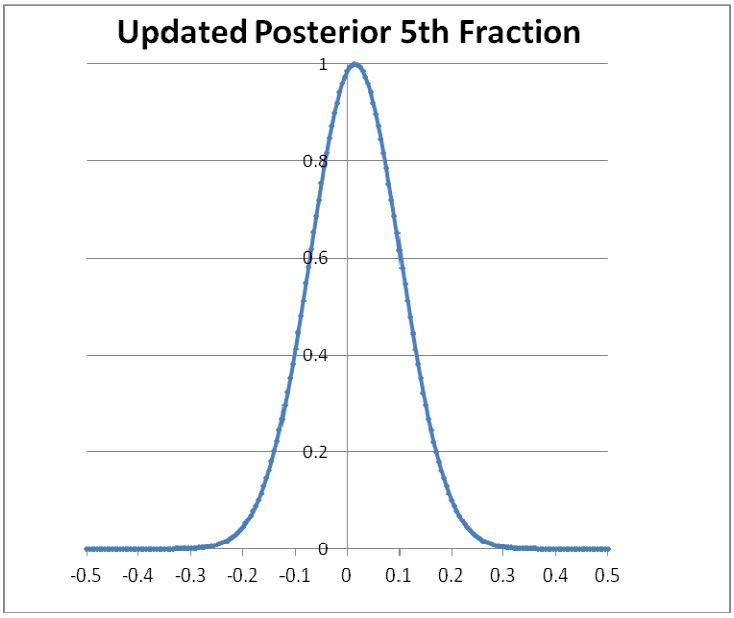

Figure 3.15 Posterior Distribution for Patient CCF 113, Y-model

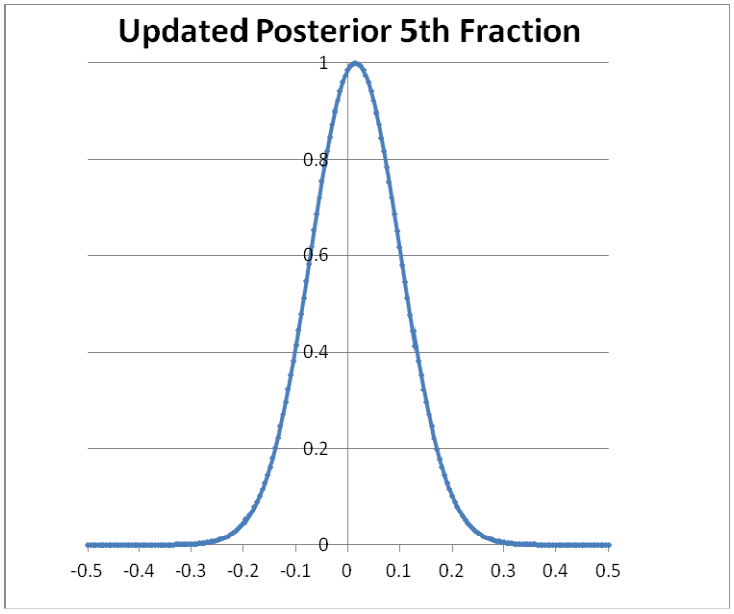

Figure 3.16 Posterior Distribution for Patient CCF 115, Y-model

A review of both plots shows the Y-vector exhibits more motion than seen in the X-vector. The width of the posterior distribution is increased in both patients as comapared to the X-vector models. As previously mentioned, the increase in motion is primarily contributed to rectal gas, bladder fill rate and respiratory motion.

CCF 113 shows a relatively symmetric pattern of motion around the zero point. The margins as predicted using the 95% criteria are 2.4 and 2 mm respectively. When applying the 99% criteria the margins are increased to 2.8 and 2.5 mm. The mean for the Y-model using the 95% value are 2.36 mm and 2.46 mm. The mean increases to 2.81mm and 2.99 mm when applying the 99% value. CCF 113 is consistent with the mean of the patient population.

CCF 115 shows a similar pattern of motion over the first five fractions. This is reflected in the predictive margins. The 95% model estimates margins to be 2.3 mm and 2 mm. As in most cases, when the 99% criteria is applied there is an increase in the margins to 2.8 mm and 2.5 mm. These results are slightly less than the mean across all 24 patients. A summary of the results for the Y-model is provided in Table 3.11.

Table 3.14 Summary of Comparisons between Accepted Clinical Models and the Bayesian Model for the Y-vector. Values indicate % of data points falling outside the clinical margins.

Patient	2 mm	6/4 mm	Bayes 95	Bayes 99
101	.25	0	1.5	.17
102	5.5	.07	16.1	9.3
103	2.8	.07	.14	.08
106	7.7	.01	3	.67
108	.61	0	0	0
109	8.9	.08	2.9	.71
110	8.7	.02	6	3.3
111	7.1	.03	4.1	1.6
112	.82	0	.05	0
113	.39	0	.64	.12
114	7.4	.78	6.9	4.6
115	16.9	.16	3.6	1.8
116	12.8	.22	9.5	4.8
117	14.4	.57	.52	.32
118	14.7	.04	5.2	5.1
119	4.5	.65	3.8	3.8
120	.31	0	.18	.03
123	14.4	.25	2.3	.59
124	10.6	.21	18.7	18.7
125	5.6	.3	1.7	1.2
126	7.1	.02	7.8	6.2
129	13.7	.28	7.7	2.3
130	6.6	.18	3.3	1
131	8.9	.24	15.2	11.4

The results of the clinical comparisons for the Y-model show strong similarities with the Polynomial approach. There is improvement between the 95% and 99% models on seven patients. The CFD did not perform well for the Y-vector and is not considered an option in modeling motion in the anterior/posterior directions.

A review of the 95% data shows that threee patients were unacceptable. CCF 102 had 16.1% of the data fall outside of the treatment margins. This result is identical to the Polynomial model. However, when the 99% criteria is applied, CCF 102 falls into the marginal category with 9.3% falling outside of the margins. CCF 124 and 131 also were unacceptable when using this approach. Even with the 99% criteria, they did improve from unacceptable. These results were consistent with the Polynomial model as well for both patients.

A review of the 99% model shows that two patients are unacceptable with respect to the established criteria. The results are equivalent to the Polynomial model. Several patients have a slightly higher rate of data points falling outside the margins but the Bayesian approach has slightly smaller margins averaged over 24 patients versus the Polynomial model when using the 95% or 99% data.

3.3.3 Bayesian, Z-model

The Bayesian Z-model shows comparable motion patterns as seen in the Y-model. The Polynomial model had over 91% of the patients score as acceptable, while the CFD approach had only 70% using the 95% criteria. Issues such as rectal gas and bladder fill will pose the same problems with the model accurately predicting motion in this direction. Figures 3.17 and 3.18 represent the Posterior distribution for two of the 24 patients presented for review.

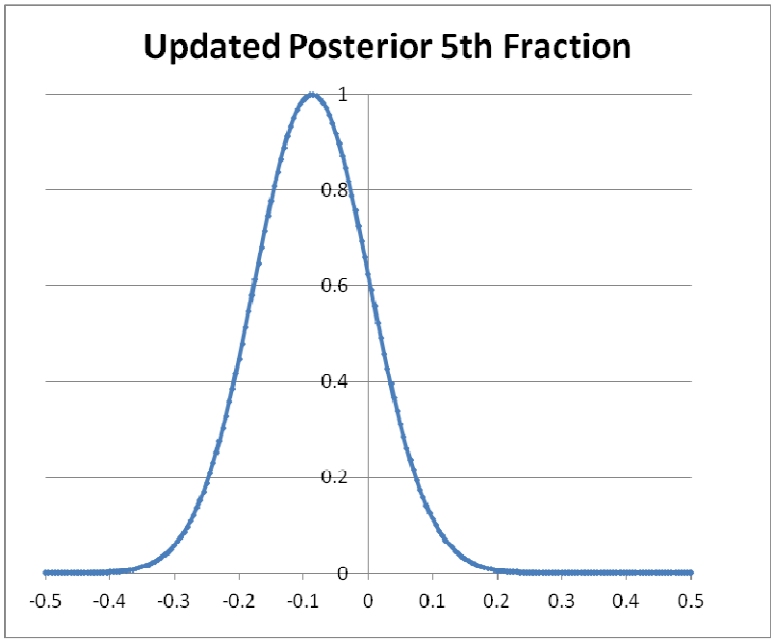

Figure 3.17 Posterior Distribution for Patient CCF 119, Z-model

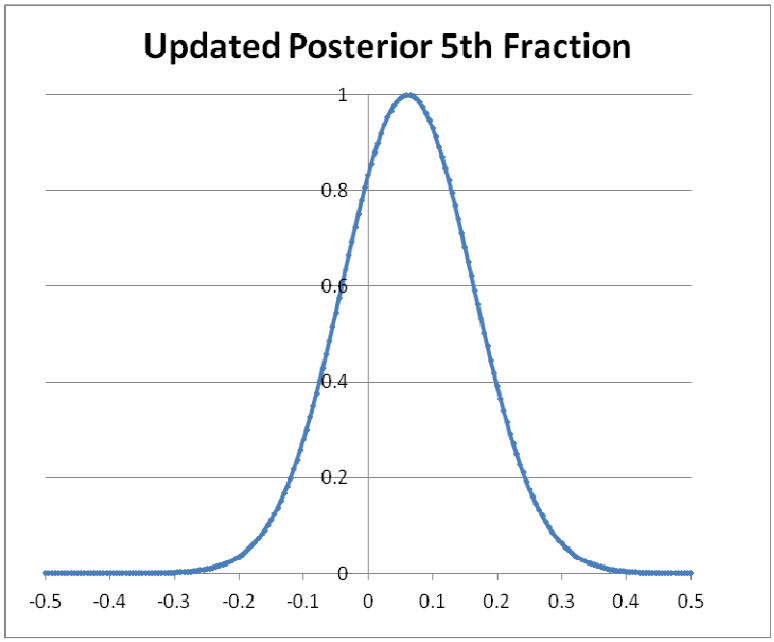

Figure 3.18 Posterior Distribution for Patient CCF 125, Z-model

A review of both plots shows that the Z-vector exhibits motion similar to the Y-vector. The width of the posterior distribution is increased in both patients as comapared to the X-vector models. The Z-vector motion can be affected by the same biological processes as the Y-vector. These processes lead to similar motion patterns between the two vectors.

CCF 119 shows a relatively asymmetric pattern of motion that is skewed to the inferior border. The margins as predicted using the 95% criteria are 1.5 mm and 3.1 mm respectively. When applying the 99% criteria the margins are increased to 1.8 mm and 3.6 mm. The mean margins for the Z-model using the 95% value are 2.38 mm and 2.54 mm. The mean increases to 2.86 mm and 3.1 mm when applying the 99% value. CCF 113 shows a superior margin well below the mean while the inferior margins are in excess of the patient population.

CCF 125 shows a more symetrical pattern over the first five fractions. This increase is reflected in the predictive margins. The 95% model estimates margins to be 3.1 mm and 1.9 mm. As in most cases, when the 99% criteria is applied there is an increase in the margins to 3.7 mm and 2.4 mm respectively. These results demonstrate margins that are in excess of the mean for the superior direction and less than the mean for the inferior motion across all 24 patients. A summary of the results for the Z-model is provided in Table 3.12.

Table 3.15 Summary of Comparisons between Accepted Clinical Models and the Bayesian Model for the Z-vector. Values indicate % of data points falling outside the clinical margins.

Patient	2 mm	6/4 mm	Bayes 95	Bayes 99
101	.24	.21	.91	.22
102	9	.02	5.3	.87
103	4.3	.02	1.1	.47
106	15.1	.05	2.9	1.4
108	1.1	0	.08	.01
109	6.1	.45	.94	.68
110	13.3	2.4	8.4	4.8
111	6.6	.25	11.6	6.4
112	5.2	0	1.9	.1
113	.83	.01	3.2	3.2
114	9.6	.57	9.3	6
115	17.9	.03	3	.69
116	16.9	.12	1.4	.4
117	14.1	.69	1.7	1
118	8.6	0	2.7	.64
119	21.2	.09	13.1	8.7
120	.31	0	.12	0
123	7.2	.01	3.5	3.3
124	6	0	6.1	5
125	10.4	.55	4	2.7
126	8.2	.03	7.3	5.4
129	5.7	.02	5.3	3.6
130	2.4	.54	1.6	1.4
131	20.7	.3	22.6	13.8

The results of the clinical comparisons for the Z-model show strong similarities with the Polynomial approach. There is improvement between the 95% and 99% models on 23 patients. The CFD did not perform well for the Z-vector and is not considered an option in modeling motion in the superior/inferior motion.

A review of the 95% data shows that threee patients were unacceptable. CCF 111 had 11.6% of the data fall outside of the treatment margins. This result is larger than seen in the Polynomial model. However, when the 99% criterion is applied, CCF 111 falls into the marginal category with 6.4% falling outside of the margins. CCF 119 and 131 also were unacceptable using this model. Even with the 99% criteria, CCF 131 did not fall into the acceptable or marginal range. CCF 119 did move to a marginal score with 8.7%. These results were consistent with the Polynomial model as well for both patients.

A review of the 99% model shows that only one patient was unacceptable with respect to the established criteria. The results are equivalent to the Polynomial model. CCF 131 was unacceptable across both models. This result is indicative of a bad data sampling over the first five fractions. The Bayesian approach has smaller margins averaged over 24 patients versus the Polynomial model when using the 95% or 99% data.

3.3.4 Summary of Bayesian Model Results

The Bayesian approach which incorporates a prior and likelihood function to compute a posterior density is the third model developed to predict prostate motion. The first five fractions are used in determining the posterior density. The Polynomial model was acceptable across the 24 patients except for an unacceptable result in two patients. The CFD did not perform well and is not considered to be a plausible approach to this research.

A total of 24 patients were modeled with the Polynomial approach. These same patients were then compared directly to the Bayesian approach to see how the models performed based on the same data. The results show that they are the same when comparing the percentage of data points that fall outside of the margins. In general, the Bayesian approach delivered comparable results with smaller overall margins. This is significant in that the reduced margins will lead to a lower volume of normal tissue irradiation. In addition, this can reduce the risk to secondary cancers.

The X-model followed a similar pattern as seen the Polynomial and CFD approaches. This pattern is a result of a general lack of motion in the lateral direction for the prostate. A baseline value of 1.5 mm has been chosen as the threshold for the model when smaller margins are predicted. This is necessary in order to account for accuracy of setup and immobilization. The fact that all three models converged on the lack of motion and the results of this approach across the patient population support it, a uniform model is most likely needed for the X-vector.

The X-model results for the Bayesian model are almost identical to the Polynomial approach. The only difference is that there is one additional patient in the 5-10% range of marginal as opposed to the 0-5% range. This is minimal and doesn't affect the outcomes of the model. The 1.5 mm margins were determined from the beginning and it is important to note that those margins might need to be changed when developing a uniform clinical model for clinical use. The reduction of 6 mm to 1.5 mm is clinically significant and should have an impact on the Dose Volume Histogram (DVH) analysis.

The results for the Bayesian Y-model show almost identical numbers as the Polynomial model. This has no clinical impact. As previously mentioned, the results are similar but the margins are generally smaller on the Bayesian model as shown in previous tables. This offers a clinical advantage while still maintaining equivalent tumor coverage. The Bayesian model for the Y-vector appears to be superior to the Polynomial and CFD approaches.

The results for the Z-model using the Bayesian approach are mixed when compared to the Polynomial approach. The 99% model is very similar except for a difference in one patient. The Bayesian 95% does not perform as well by a total of two patients. The overall margins continue to be smaller for the Bayesian Z-model (i.e. shown in previous tables) and thus make it a better treatment option. In addition, the possibility of introducing an informative prior when enough data is available could potentially improve the model in the long term.

3.4 Correlation Analysis

The methods and theory behind the correlation analysis were presented in Chapter 2. While a full analysis of all 24 patients is beyond the scope of this research, a limited analysis of several patients will provide an insight into the modeling process. The primary purpose of correlation analysis is to determine whether the motion of the prostate is inter-related to different vector components. If a particular vector model shows no correlation with the other directions (X,Y,Z), it is probable that a uniform model or independent model could be developed.

A total of three patients have been chosen to review in this section. Although two of the patients were chosen randomly, one patient was not. CCF 131 was chosen due to the fact that all predictive models were unacceptable according to accepted criteria. The correlation on this particular patient would help to determine whether there is something unique to that patient or the results are similar to other patients. The review will be based on comparing the first five fractions since the predictive margins are determined with this dataset. Then, there will be a review of the remaining 33 fractions to see if there is a measurable change in the correlation.

3.4.1 Analysis of Patient Results

A total of three patients are reviewed for their correlation. The Pearson coefficient will be the factor that is compared between the patients. In addition, the p-value will be discussed. Table 3.13 summarizes the results for the initial five fractions for each of the three patients presented.

Table 3.16 Summary of Correlation Analysis for First Five Fractions

		Pearson			**p-value**	
	X-Y	**X-Z**	**Y-Z**	**X-Y**	**X-Z**	**Y-Z**
CCF 101	-.16	-.15	.77	0	0	0
CCF 111	-.38	-.48	.54	0	0	0
CCF 131	-.19	.24	.27	0	0	0

From the three patients shown, the p-value confirms that the results are significant. In addition, there is a negative correlation between the X-vector and Y-vector across all patients. This result is mixed with respect to the X and Z-vector. CCF 131 shows a positive correlation. This result is classified as fair per the criteria set forth in Chapter 2. The results do confirm a positive correlation between the Y and Z-vectors across all patients. This supports results presented in Chapter 3. The lack of correlation with the X-vector supports the theory that lateral motion is independent of other motion and the model can be independent. The results of the remaining 34 fractions are presented in Table 3.14.

Table 3.17 Summary of Correlation Analysis for Remaining 34 Fractions

		Pearson			**p-value**	
	X-Y	**X-Z**	**Y-Z**	**X-Y**	**X-Z**	**Y-Z**
CCF 101	.018	-.078	.16	0	0	0
CCF 111	-.11	.090	.23	0	0	0
CCF 131	-.024	-.060	.66	0	0	0

The results shown above indicate a reduced correlation of motion over all three vectors. The X-vector still indicates little to no correlation between the Y and Z-vectors. The Y-Z vector shows correlation over all three patients but it is not strong except for CCF 131 (Khan, 2012). The .656 value is an increase over the .273 seen in the first five fractions.

In general there is not a definitive result from the three patients reviewed. There appears to be a lack of correlation between the X and the other vector components for all patients. This is supported in the predictive modeling as well. The correlation between the Y and Z vectors is present but not strong except for CCF 131. A qualitative review of the data used for modeling shows this correlation in a number of cases but it is evident that this might not be valid for all patients. Further analysis is warranted in determining the effects of motion and how this plays into the modeling process.

Chapter 4

Model Implementation and DVH Analysis

4.0 Model Overview

The reasoning behind this research is two-fold. First, it is necessary to determine if prostate motion is predictable. That was accomplished by using several statistical approaches that divided prostate motion into three distinct vector models. A separate model was developed for each vector using the first five fractions of data. The developed margins were then applied to the remaining 33 fractions to determine the effectiveness of the model. The results presented in Chapter 3 validate the Bayesian statistical method as the most effective model. The Bayesian approach accurately predicts margins without using too large or too small margins. The second point of this research is that if you develop predictive margins, will it make a clinical difference for the patient? The potential clinical impact is what will change the way radiation therapy is delivered. This approach will reduce the dose to the bladder and rectum while maintaining equivalent dose to the prostate will result in less complications and side effects. In addition, it will reduce the amount of normal tissue irradiated during treatment. This can lead to a reduction in secondary cancers.

4.1 Treatment Planning Process

As previously discussed, it is necessary to compare the performance of the predictive margins with clinically accepted margins in order to measure the clinical impact. This was accomplished so that the most direct comparison could be made. The initial step was to take a CT data set from a patient that has been obtained for treatment planning. The CT scan represents a patient who has no distinct anatomical issues and is of average

height and weight. The prostate along with rectum and bladder were contoured by a Board Certified Radiation Oncologist. These contours are then verified by the medical dosimetrist for completeness.

Chapter 3 discusses two clinical models, 2 mm and the 6/4 mm margin. The results over the group of 24 patients demonstrate that a 2 mm margin is not clinically acceptable due to the amount of time that the prostate exceeds the margins. Therefore, the model comparison in this section will focus on the 6/4 mm versus the Bayesian model. The Pinnacle treatment planning system was used for all treatment planning on the 24 patients. This system is an FDA 510k cleared planning system that is comparable to all other commercial treatment planning systems. Since IMRT is considered standard of care, it was used as the method of treatment delivery in the planning process.

The medical dosimetrist expands the margins around the prostate using the treatment planning algorithm that requires the expansion to be done in the (X,Y,Z) directions. The margins are first expanded using the 6/4 mm model. Once those margins are completed, an IMRT plan is developed to deliver a dose of 78 Gy over a course of 38 fractions. This results in a daily dose of 200 cGy. The IMRT plan is an optimization process that is performed by the Pinnacle TPS. The user inputs criteria at the beginning and the computer then determines the best method of delivery. In order to minimize variations in the plan comparison, all inputted criteria is identical for either the standard margins or Bayesian plan.

Once the IMRT plan has been generated, the dosimetrist verifies planning accuracy and clinical acceptability. In every case of an inverse optimization plan, there has to be minor adjustments to the plan in order to make it clinically acceptable. This adjustment can be a different weighting to a beam or an optimization parameter.

These adjustments are not significant to the overall plan and do not change the comparison results. Once the plan is considered clinical acceptable, a Dose Volume Histogram (DVH) is generated for analysis. For the purpose of this research, the DVH includes dose to the bladder and rectum. This process is then duplicated with the only difference being the predictive margins as determined by the Bayesian model.

The DVH is analyzed at varying dose levels in order to quantify the reduction across high, mid and low levels of dose. The 70 Gy threshold is considered the high dose value that has impact with complications such as rectal bleeding and late term complications. The 50 Gy dose is the mid level dose used and is an indicator of potential late term complications. The lower threshold is the 20 Gy value. Although low levels of dose are not as critical to acute reactions, they are a concern for secondary cancers and overall late term effects.

4.2 DVH Analysis

The 6/4 mm margin plan will be referred to as the base plan. The base plan is what is considered standard of care for patients being treated with the Calypso system in current radiation oncology practices. Once the IMRT plan has been generated using the base plan margins, the generated DVH will be used as the basis for comparison against the 24 research patients. The base plan is represented by the solid line. The Bayesian IMRT plan is represented by dashed lines. Figure 4.1 and 4.2 show sample DVH comparison graphs. The DVH is used in determining if a plan is acceptable from a clinical perspective.

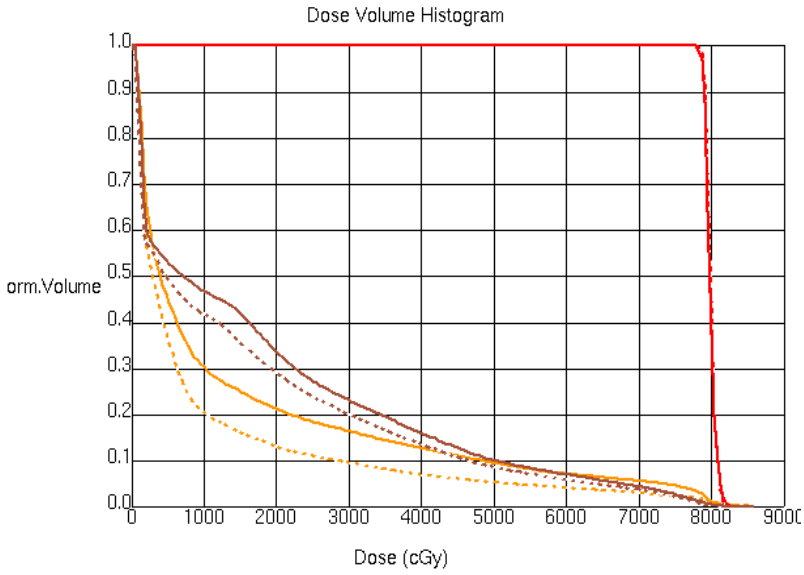

Figure 4.1 DVH for Patient CCF 101

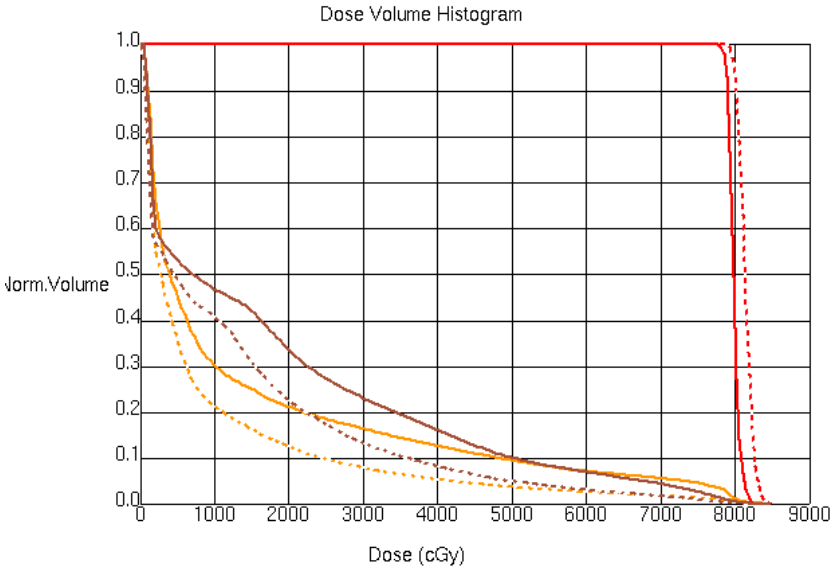

Figure 4.2 DVH for Patient CCF 130

The figures above give a visual aspect to the volume reduction when incorporating predictive margins. Both patient CCF 101 and 130 show volume reductions across the range of doses for both the rectum and bladder. The rectum is colored in brown and the bladder in burnet orange. Table 4.1 gives the DVH values associated with the rectal bladder doses as calculated when using the base plan.

Table 4.1 Base Plan Showing % Volume Receiving Given Dose

	70 Gy	**50 Gy**	**20 Gy**
Rectum	4.1	9.88	33.25
Bladder	5.35	9.27	20.97

The DVH values listed in Table 4.1 are exclusive to the anatomy and plan developed for the specific patient in this research. The doses are considered a baseline with which the Bayesian model will be compared against. To see the full table of DVH data for each patient please refer to the Appendix for further information. In order to simplify the results, each patient will be listed with the corresponding % reduction in volume for each of the dose levels shown in Table 4.1. A summary of the results are presented in Table 4.2.

Table 4.2 Summary of % volume reduction for all 24 patients in comparison to the base plan

Patient		**Rectum**			**Bladder**	
	70 Gy	**50 Gy**	**20 Gy**	**70 Gy**	**50 Gy**	**20 Gy**
101	17.8	14.7	13.1	48.8	45.2	38.6
102	27.3	47.1	7.8	46.9	10.2	32.3
103	0	2.8	14.7	43.9	38.5	27
106	63.2	14.7	13.1	70.8	62	41.2
108	36.6	25.1	2.7	18.7	21.2	9.9
109	26.8	19	10.2	50.1	43.1	34.9
110	48.8	36.6	32.8	46.3	42.8	37.5
111	21	23.4	32.8	57.1	49.2	40.7
112	36.6	30.2	25.3	53.4	47.1	41.3
113	56.8	43	30.4	66.5	59.8	48.6
114	35.4	25.7	62.3	54.6	47.5	23.5
115	37.8	31	25.3	53.1	46.8	40.8
116	24.4	20.1	27.4	53.4	46.8	41.3
117	4.9	10.7	22.6	48.9	42.7	40
118	26.8	24.1	23.2	60	52.5	43.7
119	21.2	23.7	24.4	55.7	48.5	42.3
120	34.1	29.1	25.3	53.3	47.3	42.3
123	27.3	24.5	23.8	58.7	51.3	43.7
124	37.8	30.2	25.3	58.7	51.4	42.8
125	29.3	26.1	25.3	49.5	44.4	41.3
126	24.4	25.1	25	54.9	48.2	42.3
129	19.5	23.1	22.3	54.8	48.2	42.8
130	29.3	26.1	24.7	52.5	46.5	42.3
131	44.9	33.1	20.8	55.7	49.6	41.3
Mean	30.5	25.4	23.4	52.8	45.4	38.4

Table 4.2 shows a significant reduction in dose to a given volume over the full range of 24 patients. Based on the Bayesian predictive margins, there is an average volume reduction of 30.5% receiving 70 Gy for the rectum. This is followed by slightly smaller reduction for the 50 and 20 Gy values. All patients realized a reduced volume except for CCF 103. In that instance, the predictive margins did not reduce the high dose region but did show minimal volume reduction across other dose levels. The volume reduction for the rectal doses will have a significant clinical impact on patients. This reduction will lead to less acute complications while reducing the potential for late term effects, including secondary cancers.

The volume reduction with regards to the bladder is larger than the rectal values. This is due to the location of the anterior rectal wall with relation to the prostate. The bladder when filled, will push more of the organ out of the field and thus have a potential for greater volume reduction. Over the 24 patients, the average volume reduction for the 70 Gy dose is 52.8%. Patient CCF 106 had a reduction in excess of 70%. Only one patient had less than 40% reduction, CCF 108. The mid and low dose ranges also had measured reduction in volumes.

In summary, there is large reduction in the rectal and bladder volumes receiving dose across all patients. The use of predictive margins reduces the risk of acute and late term complications. In addition, the reduction in overall dose to the critical structures has the potential to reduce the risk of secondary cancers (Gill, 2011).

Chapter 5

Conclusions

5.0 Overview

This research has focused on three approaches to developing a method that will accurately predict treatment margins for prostate cancer patients. Developing predictive margins allows for less normal tissue to be irradiated and reduces the overall risk for secondary cancers. There is growing interest in the oncology community to reduce radiation dose whether it is through diagnostic or therapeutic procedures. Currently all patients are treated with uniform margins (Van Herk, 2000).

5.1 The Polynomial Model

The initial model was an 8^{th} order polynomial. The 95% and 99% predictive lines were applied to the first five fractions and the resulting margins were used for clinical purposes. These margins were then analyzed against the remaining 34 fractions to determine if the model was acceptable, marginal or unacceptable. The Polynomial model performed well based on the results. The X-model scored acceptable in 21 of the 24 patients. A threshold of 1.5 mm was applied when the model indicated small margins that would not be clinically deliverable. The Y-model had similar results as well. When using the 99% criteria, a total of 19 patients had acceptable results. There were only three unacceptable results out of the 24 patients. The Z-model showed satisfactory results as well. A total of 20 patients scored acceptably with only three patients scoring unacceptably. The unacceptable results in both the Y-model and Z-model are direct results of patients not showing similar motion patterns in the first five fractions versus the remaining fractions. Suggestions on how to deal with this issue will be presented later. The Polynomial is an acceptable model for predictive

margins. The vast majority of patients performed well and the resulting predictive margins lead to greatly reduced volumes of normal tissue that needs to be treated.

5.2 The CFD Model

The CFD approach did not result in acceptable margins. It was initially thought that using the actual data, might lead to better estimates. This simplified statistical method did not function well over the patient population. The results for the X-model matched the Polynomial approach due to the model threshold being implemented in the vast majority of cases. The Y-model at had 10 patients score in the acceptable range when using the 99% criteria. This is not acceptable for clinical implementation. The Z-model scored slightly better in that 15 patients scored acceptably when using the 99% model. Overall the CFD model appears to be insufficient in developing patient specific margins. It is not recommended for patient treatment.

5.3 The Bayesian Model

The third model developed was the Bayesian approach. The posterior density is calculated using a likelihood function and a prior. Since the majority of prostate motion follows a Gaussian distribution (Khan, 2008), it was used as the likelihood function. For the purposes of this research, a uniform prior was implemented. The Bayesian model appears to be very effective at modeling prostate motion. The X-model results match that of the Polynomial as well as CFD approaches. Based on the results of this research, a uniform X-model is recommended across all patients. There is a lack of motion in the lateral directions and the motion that is present is minimal. These results indicate that uniform margins at significantly reduced sizes can be effectively utilized as acceptable clinical margins. The Y-model matches the results of the Polynomial approach. A total of 19 patients scored acceptable results using the 99% criteria. The main difference between

the Polynomial and Bayesian methods is that the Bayesian model had equal results with margins that were smaller. This will result in a direct clinical advantage to the patient over the course of treatment. The performance of the Z-model was slightly less than the Polynomial approach. A total of 19 patients had acceptable results. Although it resulted in one less patient having acceptable results, the overall margin reduction between the two models makes the Bayesian approach more effective from a clinical perspective.

Based on the results of this research, the Bayesian model is the best approach to develop patient specific treatment margins for prostate cancer. A balance between too small and too large of margins is accomplished with the posterior density. Through proper data collection, modeling and implementation, predictive margins can greatly reduce dose to normal tissue and reduce the risks associated with secondary cancers.

5.4 DVH Summary

The Bayesian model has shown the best results with minimal margins in predicting prostate motion across the population of 24 patients. The ability to model the motion is alone not sufficient to determine the clinical efficacy of this model. The DVH was generated across all 24 patients in order to compare the clinical results of a standard 6/4 mm model versus the predictive margins as determined by the Bayesian method.

There is significant reduction in irradiated volume across all dose levels for both the rectum and bladder. This is accomplished while maintaining equivalent dose to the prostate gland itself. All patients realized a dose reduction with their associated predictive margins. The amount of reduction was more than anticipated and indicates that this approach will have a substantial clinical impact. In addition to reducing dose to critical

structures, there is a potential to allow for dose escalation to the prostate while maintaining acceptable dose to the rectum and bladder.

Chapter 6

Future Work

6.0 Areas for Additional Work

The scope of this research was to determine whether prostate motion was patient specific or uniform across a population. If specific, then could it be modeled? Those questions were answered along with an in-depth analysis. However, there are additional areas that can be researched going forward that can greatly enhance the findings of this research.

The first area of additional work involves the determination of appropriate margins for the X-vector. This research has shown that the X-model is independent of the other models and is uniform across the population. A 1.5 mm margin was assumed for this paper. However, more analysis should be done going forward in order to determine what the optimal margins are for this type of motion.

Another area of interest would be to investigate in more detail why some patients had unacceptable results using this approach. For the X-model, a 1.5 mm margin was used as the threshold. It might be possible to establish similar thresholds for the Y and Z-vectors. These thresholds would be larger than the 1.5 mm but would reduce the effect of a bad data sampling, that results in the poor performance of the model. The basis for these margins could be on the mean values over a population sampling.

The data obtained for this study was through the Cleveland Clinic. Their work was done in close collaboration with the manufacturer Calypso. A multi-institutional study would greatly enhance the research by comparing the impact of patient setup, operational limits and greater population diversity to further validate these results as well as potentially offer areas for model improvement.

The most important area for future development would be to apply an informative prior to the posterior distribution in order to determine its impact on margins and clinical efficacy. This research assumed a non-informative prior. There is enough evidence to suggest that a well thought out informative prior based on previous patient data or even possibly modeled data can lead to better margin prediction. Additional patient analysis would be beneficial in gathering this data as well as a possible multi-institutional trial.

References

1. Beltran C, Herman M, Davis B, Planning Target Margin Calculations For Prostate Radiotherapy Based on Intrafraction and Interfraction Motion Using Four Localization Methods, Int. J. Radiation Oncology Biol. Phys., Vol. 20, No. 1 pp. 289-295, 2008.

2. Bezjak A, Bradley J, Gaspar L, Timmeman R, Lech P, Gore E, Feng-Ming P, Seamless Phase I/II Study of Stereotactic Lung Radiotherapy for Early Stage, Centrally Located, Non-Small Lung Cancer in Medically Inoperable Patients, Radiation Therapy Oncology Group, 2009.

3. Bolstad W, Introduction to Bayesian Statistics, Second Edition, 2007.

4. Booth J, Zavgorodni S, Modeling the dosimetric consequences of organ motion at CT imaging on radiotherapy treatment planning, Physics in Medicine and Biology, 46 (2001), pp. 1369-1377.

5. Bortfeld T, Jiang S, Rietzel E, Effeccts of Motion on the Total Dose Distribution, Seminars in Radiation Oncology, Vol 14, No. 1 (January), 2004, pp. 41-51.

6. Craig T, Battista J, Van Dyk J, Limitations of a convolution method for modeling geometric uncertainties in radiation therapy. Medical Physics Journal, 30 (8), 2003, pp. 2012-2020.

7. Dongarra JJ, Bunch JR, Moler CB, Stewart GW, Linpack User's Guide, SIAM, Philadelphia, 1979.

8. Elal-Olivero D, Gomez H, Quintana F, Bayesian Modeling Using a Class of Bimodal Skew-Elliptical Distributions, July 2008.

9. Fontenla E, Pelizzari C A, Roeske J C, Chen G T Y, Numerical analysis of a model of organ motion using serial imaging measurements from prostate radiotherapy, Physics in Medicine and Biology, 46 (2001), pp. 2337-2358.

10. Gill S, Thomas J, Fox C, *et al.* Acute toxicity in prostate cancer patients treated with and without image-guided radiotherapy. *Radiat Oncol* 2011;6:145.

11. Haise S Li, Int J. Rad Onc Bio, 2008.

12. Howard M, Development of Patient Specific Margins Using Intra-fractional Tracking, American Association of Medical Dosimetrists Annual Meeting, 2012.

13. Howard M, Khan MK, Miller LF, Using Mathematical Modeling to Specify Treatment Margins for Prostate Cancer May Reduce to the Rectum and Bladder, American Society of Therapeutic Radiation Oncology Annual Meeting, 2010.

14. Howard M, Miller LF, Wang Y, Underwood R, Liu T, Yang X, Yang W, Khan MK, Using Mathematical Modeling to Specify Treatment Margins for Prostate Cancer May Reduce Radiation Dose to Bladder and Rectum, ASTRO 2012.

15. Khan MK, Mahadevan A, Chen QS, Pattern of Prostate Motion, Organ Deformation and Rotation Using Real-Time Tracking and its Impact on Treatment Margins With Image Guided Radiotherapy (IGRT).

16. Khan MK, Mahadevan A, Djemil T, Vedula B, Levine L, Quantifying variations in delivered doses secondary to intrafraction prostate motion in patients treated with radiotherapy (RT) for localized prostate cancer.

17. Khan MK, Mahadevan A, Chen Q, Characterization of inter and intra-fraction prostatic motion using real-time tracking data and its potential impact on future treatment margins. Phys., Vol. 47, No. 4, pp. 1121-1135, 2000.

18. Khan MK, Yang W, Yang X, Wang Y, Howard M, Underwood R, Liu T, Prostate Motion Is Correlated in the Superior/Inferior (SI) and Anterior/Posterior (AP) Direction: Use Statistical Margin Recipes with Extreme Caution, ASTRO 2012.

19. Kleinerman RA, Tucker MA, Tarone RE, Abramson DH, Seddon JM, Stovall M, Li FP, Fraumeni JF Jr. Risk of new cancers after radiotherapy in long-term survivors of retinoblastoma: An extended follow-up. Journal of Clinical Oncology 23(10):2272-2279; 2005.

20. Landis JR, Koch GG. The measurement of observer agreement for categorical data. Biometrics. 1977; 33: 159-74.

21. Langen KM, Willoughby TR, Meeks SL, *et al.* Observations on real-time prostate gland motion using electromagnetic tracking. *Int J Radiat Oncol Biol Phys* 2008;71:1084-1090.

22. Litzenberg D, Balter J, Hadley S, Sandler H, Willoughby T, Kupelian P, Levine L, Influence of Intrafraction Motion on Margins for Prostate Radiotherapy. Int. J. Radiation Oncology Biol. Phys., Vol. 65, No. 2, pp. 548-553, 2006.

23. Lujan A, Larsen E, Balter J, Haken R, A method for incorporating organ motion due to breathing into 3-D dose calculations, Medical Physics Journal, 26 (5), 1999, pp. 715-720.

24. McCarter S D, Beckham W A, Evaluation of the validity of a convolution method for incorporating tumor movement and set-up variations into the radiotherapy treatment planning system, Physics in Medicine and Biology, 45 (2000), pp. 923-931.

25. Ott Lyman, An Introduction to Statistical Methods and Data Analysis, Third Edition, 1988.

26. Sahai H, Thompson W, AuComparisons of Approximation to the Percentil of t, X^2,Aa, and F Distributions, Au Journal of Statistical Computation and Simulation, 2974, Vole. 3, pp. 81-93.

27. Siegel R, Ward E, Brawley O, *et al.* Cancer statistics, 2011: the impact of eliminating socioeconomic and racial disparities on premature cancer deaths. *CA Cancer J Clin*;61:212-236.

28. Sigma Plot Users Guide, Systat Software, 2009.

29. Song W, Schaly B, Bauman G, Battista J, Van Dyk J, Image-guided adaptive radiation therapy (IGART): Radiobiological and dose escalation considerations for localized carcinoma of the prostate, Medical Physics Journal, 32 (7), 2005, pp. 2193-2203.

30. Tamahane A, Dunlop D, Statistics and Data Analysis, 2000.

31. Van Herk M, Remeijer P, Rasch C, Lebesque J, The Probability of Correct Target Dosage: Dose-Population Histograms for Deriving Treatment Margins in Radiotherapy, Int. J. Radiation Oncology Biol., 2000.

32. Willoughby TR, Kupelian PA, Pouliot J, *et al.* Target localization and real-time tracking using the Calypso 4D localization system in patients with localized prostate cancer. *Int J Radiat Oncol Biol Phys* 2006;65:528-534.

33. Winker R, An Introduction to Bayesian Inference and Decision, Second Edition, 2003.

34. Zietman AL, DeSilvio ML, Slater JD, *et al.* Comparison of conventional-dose vs high-dose conformal radiation therapy in clinically localized adenocarcinoma of the prostate: a randomized controlled trial. *JAMA* 2005;294:1233-1239.

Appendices

Appendix I

Coefficients for Polynomial Model

Coefficients for the Polynomial approach, X-model.

Patient	A0	A1	A2	A3	A4	A5	A6	A7	A8
101	-4.6 E-3	2.4 E-4	-6.8 E-6	3.4 E-8	6.7 E-11	-9.5 E-13	2.8 E-15	1.7 E-21	0.06
102	-5.9 E-3	1.2 E-4	-2.8 E-5	3.9 E-7	-2.4 E-9	8.1 E-12	-1.5 E-14	1.3 E-17	-4.9 E-21
103	3.7 E-3	5.7 E-6	1.1 E-5	-2.1 E-7	1.6 E-9	-6.3 E-12	1.2 E-14	4.7 E-21	.08
106	-5.2 E-3	7 E-4	2.7 E-5	-2.1 E-9	9.4 E-12	-2.4 E-14	3.1 E-17	-1.7 E-20	.38
108	.014	-2.1 E-3	3.4 E-5	-2.7 E-7	1.3 E-9	-3.4 E-12	5.5 E-15	-4.7 E-18	1.7 E-21
109	-.01	-1.4 E-3	3.7 E-5	-4.9 E-7	3.5 E-9	-1.4 E-11	3.2 E-14	-3.7 E-17	1.8 E-20
110	-1.1 E-3	-4.1 E-4	1.2 E-5	-7.8 E-8	9 E-11	3.4 E-13	6.6 E-16	-6.2 E-18	7.7 E-21
111	7.5 E-3	-3.3 E-4	-5.8 E-7	7.7 E-8	-6.8 E-10	2.6 E-12	-5.1 E-15	4.9 E-18	-1.9 E-21
112	6.1 E-3	5.3 E-4	-1.7 E-5	1.9 E-7	-7.6 E-10	2.5 E-13	6.2 E-15	-1.6 E-17	1.2 E-20
113	-5.3 E-3	1.2 E-3	-2.3 E-5	2 E-7	-8.8 E-10	2 E-12	-2.4 E-15	1.3 E-18	-2.4 E-22
114	5.9 E-3	-1 E-4	9 E-6	-1.3 E-7	1.1 E-9	-5 E-12	1.3 E-14	-1.9 E-17	1 E-20
115	-8.6 E-4	-2 E-4	1.2 E-5	-2.4 E-7	2.5 E-9	-1.4 E-11	4.2 E-14	-6.5 E-17	4 E-20
116	6.5 E-3	1.8 E-5	2.1 E-5	-3.1 E-7	2.1 E-9	-7.5 E-12	1.5 E-14	-1.6 E-17	6.5 E-21
117	-7.6 E-3	8.7 E-4	-3.5 E-5	5.5 E-7	-4.2 E-9	1.7 E-11	-4 E-14	4.7 E-17	-2.2 E-20
118	-5.5 E-3	9.5 E-4	-2 E-5	2.1 E-7	-6.1 E-10	-3.2 E-12	2.5 E-14	-5.9 E-17	4.7 E-20
119	2.7 E-3	7.3 E-4	-1.4 E-5	1.7 E-7	-1.1 E-9	3.8 E-12	-6.9 E-15	6.3 E-18	-2.3 E-21
120	-2.8 E-3	-4.7 E-4	7.6 E-6	-5.3 E-8	2.9 E-10	-1.4 E-12	4.1 E-15	-5.7 E-18	3.1 E-21
123	5.6 E-3	-1.3 E-4	1.3 E-5	-2.1 E-7	1.5 E-9	-5.3 E-12	1 E-14	-9.6 E-18	3.6 E-21
124	-4.6 E-3	2.4 E-4	-1.6 E-5	3.9 E-7	-4.5 E-9	2.8 E-11	-9.9 E-14	1.8 E-16	-1.3 E-19
125	6 E-3	-4.5 E-4	1.5 E-5	-1.5 E-7	6.8 E-10	-1.6 E-12	1.8 E-15	-8 E-19	-1.8 E-23
126	-6.4 E-3	4.3 E-4	-3.1 E-5	4.8 E-7	-3.2 E-9	1.1 E-11	-2.1 E-14	2 E-17	-7.8 E-21
129	-7.1 E-3	5 E-4	-1.6 E-5	1.9 E-7	-1.1 E-9	3.6 E-12	-6.6 E-15	6.3 E-18	-2.4 E-21
130	-7.4 E-4	1.6 E-4	1.1 E-6	-3.7 E-8	3.1 E-10	-1.3 E-12	2.9 E-15	-3.2 E-18	1.4 E-21
131	3.6 E-3	-2.3 E-3	8.3 E-5	-1.2 E-6	8.1 E-9	-3 E-11	6.2 E-14	-6.6 E-17	2.9 E-20

Coefficients for the Polynomial approach, Y-model.

Patient	A0	A1	A2	A3	A4	A5	A6	A7	A8
101	0	2.7 E-3	-5.8 E-5	6.1 E-7	-3.8 E-9	1.4 E-11	-2.9 E-14	3.1 E-17	-1.3 E-20
102	0	8.8 E-4	-2.9 E-5	3.6 E-7	-2.3 E-9	8 E-12	-1.5 E-14	1.4 E-17	-4.7 E-21
103	0	1.2 E-3	-1.4 E-6	-1.6 E-7	1.9 E-9	-8.3 E-12	1.9 E-14	-2.1 E-17	9.2 E-21
106	0	6.6 E-4	-3 E-5	6.2 E-7	-6.8 E-9	3.8 E-11	-1.1 E-13	1.6 E-16	-9.3 E-20
108	0	-1.3 E-3	2.5 E-5	-2.7 E-7	1.7 E-9	-6.2 E-12	1.2 E-14	-1.2 E-17	5 E-21
109	0	1.2 E-3	-4.5 E-5	6.9 E-7	-4.7 E-9	1.7 E-11	-3.1 E-14	2.7 E-17	-8.7 E-21
110	0	-1.2 E-4	7.4 E-5	-1.2 E-6	9.4 E-9	-4 E-11	9.8 E-14	-1.3 E-16	7.3 E-200
111	0	-1.9 E-3	5.4 E-5	-6.2 E-7	3.3 E-9	-9.9 E-12	1.7 E-14	-1.5 E-17	5.6 E-21
112	0	4.2 E-3	-5.3 E-5	-5.3 E-7	1.3 E-8	-8.1 E-11	2.5 E-13	-3.8 E-16	2.3 E-19
113	0	-2.1 E-3	6 E-5	-6.6 E-7	3.7 E-9	-1.1 E-11	2 E-14	-1.8 E-17	6.7 E-21
114	0	-6.4 E-4	8.4 E-5	-2.2 E-6	2.5 E-8	-1.5 E-10	4.5 E-13	-7 E-16	4.4 E-19
115	0	-1.2 E-3	4.9 E-5	-1.1 E-6	1 E-8	-5.4 E-11	1.6 E-13	-2.3 E-16	1.4 E-19
116	0	5.8 E-4	6.8 E-6	-1.5 E-7	6.6 E-10	-7.7 E-13	-1.4 E-15	3.8 E-18	-2.3 E-21
117	0	2.1 E-3	-1.8 E-4	3.7 E-6	-3.1 E-8	1.3 E-10	-3 E-13	3.5 E-16	-1.6 E-19
118	0	-2.9 E-3	1.5 E-4	-2.9 E-6	2.6 E-8	-1.3 E-10	3.6 E-13	-5.1 E-16	3 E-19
119	0	-2.3 E-4	1.6 E-5	-2 E-7	1 E-9	-2.7 E-12	3.7 E-15	-2.5 E-18	6.4 E-22
120	0	6.6 E-4	-4.6 E-6	-1.3 E-7	2.2 E-9	-1.2 E-11	3.5 E-14	-4.7 E-17	2.5 E-20
123	0	1.2 E-3	-2.5 E-6	-1.4 E-7	1.4 E-9	-5.5 E-12	1.2 E-14	-1.3 E-17	5.8 E-21
124	0	-1.5 E-3	6.3 E-5	-1.4 E-6	1.5 E-8	-9 E-11	2.9 E-13	-4.9 E-16	3.4 E-19
125	0	-6 E-4	1.1 E-5	-5.3 E-8	-6.6 E-11	1.1 E-12	-3.2 E-15	3.5 E-18	1.4 E-21
126	0	-6.2 E-4	8.3 E-6	-5.4 E-8	9.3 E-11	4.6 E-13	-2.4 E-15	3.9 E-18	-2.2 E-21
129	0	7.8 E-4	-3.3 E-5	4.5 E-7	-2.8 E-9	9 E-12	-1.6 E-14	1.5 E-17	-5.7 E-21
130	0	1.9 E-3	-3.3 E-5	2.2 E-7	-5.5 E-10	-5.2 E-13	4.7 E-15	-7.6 E-18	3.9 E-21
131	0	7.1 E-4	-4.8 E-5	9.1 E-7	-7.2 E-9	3 E-11	-6.7 E-14	7.9 E-17	-3.8 E-20

Coefficients for the Polynomial approach, Z-model.

Patient	A0	A1	A2	A3	A4	A5	A6	A7	A8
101	0	1.6 E-3	3.5 E-6	-2.6 E-7	1.7 E-9	-4.7 E-12	5.5 E-15	-1.9 E-18	-5.9 E-22
102	0	6.4 E-4	-5.4 E-7	-3.6 E-7	4.6 E-9	-2.5 E-11	6.7 E-14	-9 E-17	4.8 E-20
103	0	8.3 E-4	5.2 E-6	-2.4 E-7	2.3 E-9	-1 E-11	2.3 E-14	-2.5 E-17	1.1 E-20
106	0	-2.7 E-3	7.3 E-5	-6.9 E-7	1.6 E-9	8.6 E-12	-5.5 E-14	1.1 E-16	-7 E-20
108	0	6.4 E-5	4.2 E-6	-1 E-7	8.9 E-10	-3.5 E-12	7 E-15	-7.1 E-18	2.8 E-21
109	0	-1.1 E-3	-4.9 E-6	3.5 E-7	-3.3 E-9	1.3 E-11	-2.8 E-14	2.7 E-17	-9.4 E-21
110	0	-1.2 E-3	6.5 E-5	-1 E-6	7.9 E-9	-3.4 E-11	8.3 E-14	-1.1 E-16	5.9 E-20
111	0	6.3 E-4	-2.3 E-6	-8.6 E-8	8.1 E-10	-3 E-12	5.8 E-15	-5.5 E-18	2.1 E-21
112	0	9.8 E-3	-2 E-4	9.5 E-7	4.4 E-9	-5.4 E-11	1.9 E-13	-2.9 E-16	1.7 E-19
113	0	1 E-4	7.5 E-8	1.9 E-8	-2.1 E-10	8.5 E-13	-1.6 E-15	1.5 E-18	-5.3 E-22
114	0	3.4 E-3	-5.4 E-5	-1.8 E-7	8 E-9	-6 E-11	2.1 E-13	-3.5 E-16	2.3 E-19
115	0	-7.2 E-4	2 E-5	-6.8 E-7	8.1 E-9	-4.6 E-11	1.4 E-13	-2.2 E-16	1.3 E-19
116	0	-4.6 E-3	1.5 E-4	-1.9 E-6	1.1 E-8	-3.8 E-11	6.9 E-14	-6.7 E-17	2.6 E-20
117	0	2.6 E-3	-1.4 E-4	2.7 E-6	-2.1 E-8	8.6 E-11	-1.8 E-13	2 E-16	-8.7 E-20
118	0	-1.3 E-3	6.3 E-5	-1.3 E-6	1.2 E-8	-5.2 E-11	1.1 E-13	-1.2 E-16	4.6 E-20
119	0	-1 E-3	5.70E -5	-9.40E-7	6.3 E-9	-2.1 E-11	3.8 E-14	-3.5 E-17	1.3 E-20
120	0	-1.3 E-3	2.5 E-5	-3.2 E-7	2.3 E-9	-9.2 E-12	2 E-14	-2.3 E-17	1 E-20
123	0	-1.5 E-4	5.4 E-6	-1.6 E-7	1.4 E-9	-5.8 E-12	1.3 E-14	-1.4 E-17	6.4 E-21
124	0	1.4 E-3	-5.7 E-5	8.6 E-7	-7.9 E-9	4.6 E-11	-1.6 E-13	3 E-16	-2.3 E-19
125	0	-4.1 E-4	2.1 E-5	-2.7 E-7	1.6 E-9	-4.8 E-12	7.4 E-15	-5.8 E-18	1.7 E-21
126	0	1..1 E-3	-2.5 E-5	1.7 E-7	-2.9 E-10	-1 E-12	4.8 E-15	-7 E-18	3.4 E-21
129	0	-2.6 E-4	-8.4 E-6	1.6 E-7	-1.1 E-9	4 E-12	-7.7 E-15	7.4 E-18	-2.8 E-21
130	0	2 E-3	-7.5 E-5	10 E-7	-6.1 E-9	1.9 E-11	-3.4 E-14	3.1 E-17	-1.1 E-20
131	0	-2.5 E-4	-2 E-5	6.6 E-7	-6.3 E-9	2.8 E-11	-6.6 E-14	7.7 E-17	-3.6 E-20

Appendix II

Parameters for Bayesian Model

Bayesian Parameters for X-model

Patient	Mean	Variance	St Dev.
101	-.007	.0011	.033
102	-.085	.0059	.077
103	.018	.0034	.058
106	-.00073	.00071	.027
108	-.012	.0064	.08
109	.0074	.021	.14
110	.012	.003	.055
111	-.029	.0037	.061
112	.061	.021	.14
113	.019	.007	.09
114	.02	.0078	.088
115	-.0033	.00076	.027
116	.04	.002	.045
117	.019	.027	.16
118	.03	.0008	.028
119	-.017	.003	.056
120	-.015	.00038	.019
123	-.087	.005	.071
124	-.019	.0012	.035
125	.032	.0015	.038
126	-.035	.0047	.069
129	.003	.0009	.03
130	.017	.002	.044
131	-.019	.0025	.05

Bayesian Parameters for Y-model

Patient	Mean	Variance	St Dev.
101	.003	.009	.097
102	-.015	.0031	.055
103	.038	.019	.14
106	-.069	.0092	.096
108	.044	.019	.14
109	.03	.011	.10
110	.086	.0077	.087
111	-.077	.008	.09
112	.011	.009	.097
113	.015	.0075	.086
114	.015	.0075	.086
115	-.0033	.00076	.027
116	-.085	.0079	.089
117	-.013	.052	.23
118	-.081	.0053	.072
119	-.037	.003	.055
120	.031	.0074	.086
123	-.011	.013	.11
124	-.04	.0013	.036
125	.031	.015	.12
126	-.063	.0049	.07
129	.028	.0087	.093
130	-.017	.0095	.097
131	.03	.0043	.065

Bayesian Parameters for Z-model

Patient	Mean	Variance	St Dev.
101	.017	.011	.11
102	-.035	.0064	.08
103	.0098	.013	.11
106	-.067	.012	.11
108	.07	.013	.11
109	.007	.021	.14
110	.025	.009	.097
111	-.03	.004	.061
112	.06	.021	.15
113	.02	.008	.09
114	.02	.008	.09
115	-.09	.01	.1
116	-.02	.02	.15
117	.018	.027	.16
118	-.09	.008	.089
119	-.03	.015	.12
120	-.018	.015	.12
123	-.087	.005	.07
124	-.056	.004	.063
125	.061	.01	.1
126	-.03	.005	.069
129	-.045	.005	.071
130	-.03	.013	.11
131	.027	.0074	.086

Vita

Michael Edward Howard was born in Silver Spring, MD on November 19, 1969. His family moved to Clearwater, FL in 1975. In June of 1988, he graduated from Pinellas Park High School in Largo, FL. He transferred from the University of South Florida to the University of Tennessee in May1990. In December 1992 he received his Bachelors Degree in Nuclear Engineering. In May of 1995 he received is Masters of Science Degree in Radiological Engineering. He became board certified in radiation therapy physics by the American Board of Medial Physics in May 2001. In January of 2008 he enrolled in the Doctoral program in Nuclear Engineering. In December of 2012 he received his Doctor of Philosophy in Nuclear Engineering.